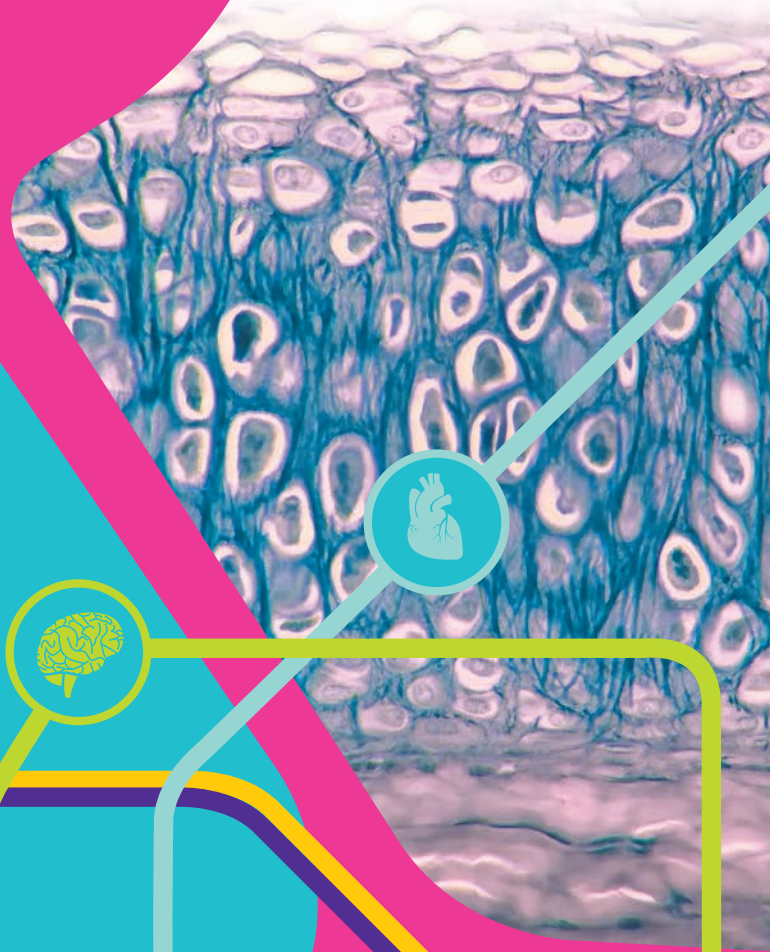
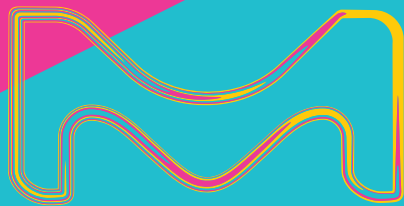


Material Matters™

VOLUME 13 • NUMBER 3



Mapping the Future Advances in Tissue Engineering

PHOTO-CROSSLINKABLE GELATIN HYDROGELS: Versatile Materials for High-Resolution Additive Manufacturing

CONTROLLED FABRICATION METHODS for Tissue Engineering Constructs

POLY(ETHYLENE GLYCOL) (PEG) AND SYNTHETIC PEG DERIVATIVES for Tissue Engineering and Cell Delivery



The life science business of Merck KGaA, Darmstadt, Germany operates as MilliporeSigma in the U.S. and Canada.



Introduction



Brianna Upton, Ph.D.
Product Manager,
Biomedical Materials

Welcome to the final issue of Material Matters™ for 2018, focused on recent advancements in tissue engineering research. This issue highlights new and innovative materials and techniques for addressing critical issues in the development of functional tissues and organs for regenerative medicine applications.

Gelatin has been routinely used in tissue engineering applications due to its ability to interact with cells and allow for matrix remodeling, but its thermo-reversible gelation limits its applications *in vivo*. In our first article, Professor Van Vlierberghe (Ghent University, Belgium) discusses synthetic modifications to gelatin, improving the three-dimensional (3D) print resolution and resulting material properties.

While the advancement of biomaterials has led researchers closer to the ability to create functional replacement organs, new materials alone are not enough to reach this goal. In our second article, Professor De Laporte (Leibniz-Institute for Interactive Materials, Germany) highlights existing and novel fabrication methods for both solid and hydrogel-based scaffolds for tissue engineering applications.

Natural materials have a highly varied structure, making it difficult to utilize them in applications that require precise degradation rates and mechanics. With its cytocompatibility, minimal immunogenicity, and hydrophilicity, poly(ethylene glycol)-based (PEG) hydrogels are frequently used as synthetic scaffolds. In our final article, Professor Hoare (McMaster University, Canada) highlights new synthetic modifications of PEG to improve the mechanical properties and degradation of resulting hydrogels in tissue engineering applications.

In this issue, each article is accompanied by a list of polymers and related products available from the Sigma-Aldrich® portfolio. Please visit SigmaAldrich.com/matsci for additional product offerings and information. As always, please bother us with new product suggestions and your feedback at matsi@sial.com.



About the Cover

As a subfield of regenerative medicine, tissue engineering utilizes the combination of scaffolds, cells, and bioactive molecules to generate physically relevant, functional tissues and organs. While new materials and techniques have helped to rapidly advance the field, the goal of creating complex organs has not yet been achieved. This issue's cover illustrates how new advancements are allowing researchers to reach previously unattainable goals in tissue engineering.

Merck KGaA, Darmstadt, Germany
Frankfurter Strasse 250
64293 Darmstadt, Germany
Phone +49 6151 72 0

To Place Orders / Customer Service

Contact your local office or visit
SigmaAldrich.com/order

Technical Service

Contact your local office or visit
SigmaAldrich.com/techinfo

General Correspondence

Materials Science
materialsscience@sial.com

Subscriptions

Request your FREE subscription to *Material Matters*™ at SigmaAldrich.com/mm

The entire *Material Matters*™ archive is available at SigmaAldrich.com/mm

Material Matters™ (ISSN 1933-9631) is a publication of Merck KGaA, Darmstadt, Germany

Copyright © 2018 Merck KGaA, Darmstadt, Germany and/or its affiliates. All rights reserved. MilliporeSigma, the vibrant M, Sigma-Aldrich and Material Matters are trademarks of Merck KGaA, Darmstadt, Germany or its affiliates. All other trademarks are the property of their respective owners. Detailed information on trademarks is available via publicly accessible resources. More information on our branded products and services on MilliporeSigma.com

Your Material Matters



Bryce P. Nelson, Ph.D.
Materials Science Initiative Lead

We welcome fresh product ideas. Do you have a material or compound you wish to see featured in our Materials Science line? If it is needed to accelerate your research, it matters. Send your suggestion to matsci@sial.com for consideration.

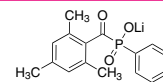
Professor Ali Khademhosseini at the University of California, Los Angeles, USA, recommended the addition of lithium phenyl-2,4,6-trimethylbenzoylphosphinate (Cat. No. **900889**) to our catalog for use in tissue engineering applications. Lithium phenyl-2,4,6-trimethylbenzoylphosphinate (LAP) is a water-soluble, cytocompatible, Type I photoinitiator used in the polymerization of hydrogels or other scaffolds in tissue engineering¹⁻⁵ applications. LAP is preferred over other photoinitiators for biological applications due to its superior water solubility and improved polymerization kinetics.¹ The improvement in polymerization kinetics enables crosslinking at lower initiator concentrations, reducing potential toxicity and increasing cell viability.^{1,2} In addition to increased polymerization rates at 365 nm, LAP also absorbs at 400 nm, allowing for polymerization with visible light, yielding cell-laden constructs with high cell viability.

References

- (1) Nguyen, K.T. & West, J.L. "Photopolymerizable hydrogels for tissue engineering applications" *Biomaterials* **2002**, *23*, 4307-4314
- (2) Ma, Y. et al. "Deterministically patterned biomimetic human iPSC-derived hepatic model via rapid 3D bioprinting" *Proc. Natl. Acad. Sci.* **2016**, *113*(8), 2206-11
- (3) Ruskowitz, E. and DeForest, C. "Photoresponsive biomaterials for targeted drug delivery and 4D cell culture" **2018**, *Nat. Rev. Mater.*, *3*, 17087
- (4) Williams, C.G.; Malik, A.N.; Kim, T.K.; Elisseff, J.H. "Variable cytocompatibility of six lines with photoinitiators used for polymerizing hydrogels and cell encapsulation" *Biomaterials*, **2015**, *26*(11), 1211-1218
- (5) Fairbanks, B.D. et al. "Photoinitiated polymerization of PEG-diacrylate with lithium phenyl-2,4,6-trimethylbenzoylphosphinate: polymerization rate and cytocompatibility" *Biomaterials*, **2009**, *30*(35), 6702-6707

Lithium phenyl-2,4,6-trimethylbenzoylphosphinate

[85073-19-4] C₁₆H₁₆LiO₃P FW 294.21



LAP
≥95%

crystalline powder

Store at 2-8°C

1g	900889-1G
5g	900889-5G

Table of Contents
Articles

Photo-crosslinkable Gelatin Hydrogels: Versatile Materials for High-Resolution Additive Manufacturing	75
Controlled Fabrication Methods for Tissue Engineering Constructs	83
Poly(ethylene glycol) (PEG) and Synthetic PEG Derivatives for Tissue Engineering and Cell Delivery	90

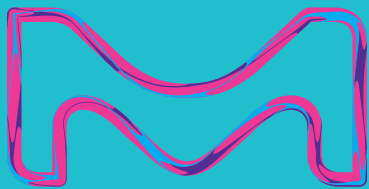
Featured Products

Gelatin A selection of gelatins, functionalized gelatins, and building blocks for gelatin functionalization	81
Natural Polymers for Tissue Engineering A list of collagens and Fibrin materials	88
Reagents for Solvent Casting A selection of materials for solvent casting	89
Synthetic Polymers for Hydrogels A selection of Polyacrylamide and PEGs	89
Functionalized POEGMA A list of functionalized POEGMA	96
Functionalized PEGs A selection of linear and multi-arm PEGs	96

creative inking

Select. Formulate. **Bioprint.**

Want to keep innovation flowing in your bioprinting research? It's easy when you team up with a leader in polymers and nanomaterials for 3D printing. Watch your research take shape with our vast selection of materials and inks ready for your printer and application.



Discover more at
SigmaAldrich.com/3dp

The life science business of Merck KGaA,
Darmstadt, Germany operates as
MilliporeSigma in the U.S. and Canada.

Photo-Crosslinkable Gelatin Hydrogels: Versatile Materials for High-Resolution Additive Manufacturing



Jasper Van Hoorick,^{1,2} Aleksandr Ovsianikov,^{3,4} Peter Dubrueel,¹ Sandra Van Vlierberghe^{*1,2}

¹Polymer Chemistry and Biomaterials Group, Centre of Macromolecular Chemistry, Ghent University, Krijgslaan 281, S4, 9000 Ghent, Belgium (www.pbm.ugent.be)

²Brussels Photonics, Department of Applied Physics and Photonics, Flanders Make and Vrije Universiteit Brussel, Pleinlaan 2, 1050 Elsene, Belgium (www.b-phot.org)

³Institute of Materials Science and Technology, Technische Universität Wien, Getreidemarkt 9 1060 Vienna, Austria

⁴Austrian Cluster for Tissue Regeneration (www.tissue-regeneration.at)

*Email: Sandra.Vanvlierberghe@ugent.be

Introduction

Gelatin has long been of interest to those in the field of tissue engineering. It is derived from collagen, the main constituent of the natural extracellular matrix (ECM) and interacts with cells through the arginine-glutamine-aspartic acid (RGD) sequences in its protein backbone, while also being enzymatically degradable.¹ Gelatin is produced as a by-product of meat production, rendering it extremely cost-effective,² and it is considered safe by the Food and Drug Association (FDA) due to its long track record in the food and pharmaceutical industries.³

Gelatin has an upper critical solution temperature (UCST) of around 30–35°C, meaning it is water soluble above this temperature and forms a hydrogel at lower temperatures.^{4–6} This temperature-dependent transformation is useful for extrusion-based rapid manufacturing (RM) technologies, as a shape introduced by extrusion from a heated nozzle can be locked in by using a cooler environment.⁷

However, this property also means that the material does not remain stable in physiological or cell culture conditions. As a result, gelatin was originally only used as a temporary cell carrier, thereby enabling a more straightforward manipulation of cells. Alternatively, it was stabilised by coupling the primary amines present in the (hydroxy)lysine and ornithine functionalities to the carboxylic acids in aspartic and glutamic acid (resulting in a crosslinked hydrogel network), or by

crosslinking nucleophilic functionalities using glutaraldehyde. These procedures are characterized by limited control over the design of 3D structures.^{3,8,9}

Fortunately, gelatin stabilization strategies took a giant leap forward in 2000 when our research group developed and patented gelatin-methacrylamide (Gel-MOD), the first photo-crosslinkable gelatin derivative, thereby enabling convenient and straightforward material processing.^{6,10} Functionalization occurs through the reaction between primary amines present in the side chains of the (hydroxy)lysine and ornithine in gelatin and methacrylic anhydride, which introduces methacrylamides.⁶ Since its introduction, this gelatin-methacrylamide has been applied for a plethora of biofabrication strategies, and is considered a gold standard in the field.^{4,7,11–17} This material, discovered in academia, is now offered commercially by several companies as a bioink for biofabrication purposes.^{18–20}

Subsequently, several other photo-crosslinkable gelatin derivatives suitable for biofabrication (**Figure 1**) have emerged. They can be subdivided into two classes based on the applied crosslinking mechanism, being either chain-growth or step-growth polymerization. This article focuses on photo-crosslinkable derivatives for biofabrication purposes that have applications in high-resolution additive manufacturing

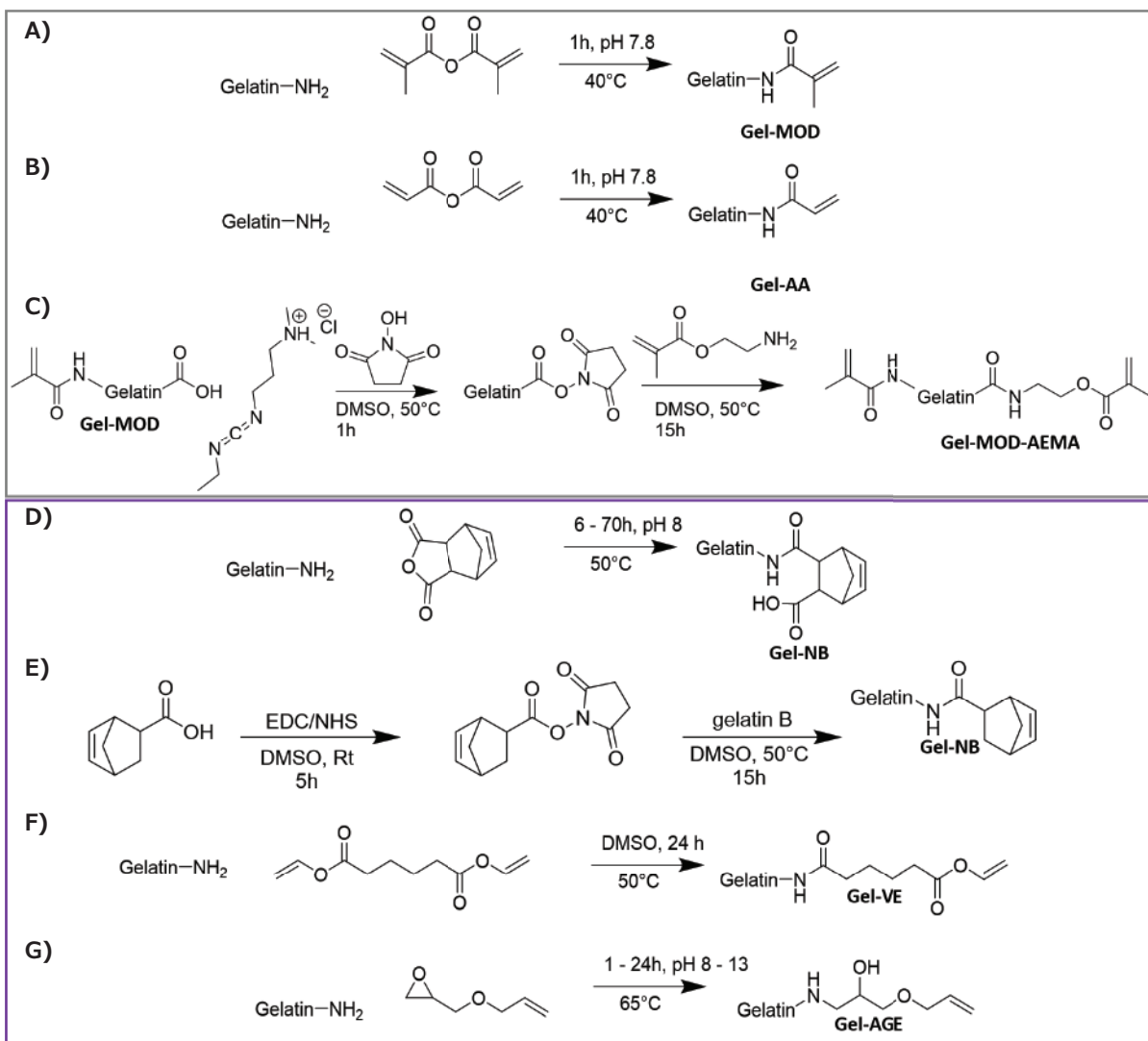


Figure 1. Overview of preparation methods of different photo-crosslinkable gelatins: chain-growth derivatives (grey, upper frame): A) Gelatin-methacrylamide (Gel-MOD),⁶ B) Gelatin-acrylamide (Gel-AA),²¹ C) Gel-MOD-AEMA,⁵ step-growth derivatives (purple, lower frame), D) Gelatin-norbornene (Gel-NB) synthesized via reaction with carbic anhydride,¹ E) Gelatin-norbornene (Gel-NB) synthesized via reaction with 5-norbornene-2-carboxylic acid,²² F) Gelatin-vinyl ester (Gel-VE),²³ G) Allylated gelatin (Gel-AGE).²⁴

Crosslinking Mechanisms

Chain-growth Crosslinking

Most crosslinkable gelatins are formed using a chain growth crosslinking approach. In this mechanism, the reactive functionalities (typically (meth)acrylates or (meth)acrylamides) immobilized on the gelatin chains are polymerized with each other, resulting in the formation of short oligomer/polymer chains between the gelatin chains (Figures 2A and C).^{5,6,11,21,22} This enables straightforward material handling, with only material dissolution and addition of a suitable photo-initiator prior to crosslinking. No crosslinking agent is required. These solutions exhibit longer stability above the UCST in comparison to thiol-ene based systems. For example, when dithiothreitol (DTT) is used as a crosslinker, its half life at pH 8.5 ranges from 11 h at 0°C to only 0.2 h at 40°C (discussed below). Gel-MOD, for example, is kept at 40°C for over 24 hours during

the modification reaction without any problems. This level of stability is typically required during additive manufacturing processes or for cell encapsulation experiments.^{5,25} Moreover, chain growth crosslinking provides stiffer hydrogels (Figure 3).²² A drawback of chain-growth crosslinking is the formation of a more heterogeneous network, which is prone to more shrinkage during crosslinking. Furthermore, the kinetic profile of free radical chain-growth polymerizations is usually more complicated because of diffusion limitations, chain-length issues, and reaction diffusion limitations resulting in termination, leading to a lower degree of control over the number of reacted functional groups.^{26,27} The crosslinking reaction is also prone to oxygen inhibition, which is a problem for use in cell encapsulation experiments and influences reaction reproducibility. Finally, a higher spatiotemporal energy is required to crosslink gelatin compared to the thiol-ene-based step-growth hydrogels discussed below.²²

Step-growth Crosslinking

The second type of photo-crosslinkable hydrogels uses a step-growth polymerisation approach to introduce crosslinks into the hydrogel. A step-growth mechanism occurs between two complementary reactive groups, which can ideally only react with each another.²⁷ The most common crosslinking chemistry applied for hydrogels following this approach is thiol-ene “photo”-click chemistry (Figure 2B). By using this methodology, networks can be formed by reacting any thiol with any ‘ene’ functionality either following a light-induced, radical-mediated thiol-ene reaction, or by the formation of an anionic species resulting in a thiol Michael-type addition.²⁷ The light-induced reaction usually proceeds via the formation of a thiol-based radical which can be generated by irradiation either in the presence or in the absence of a photo-initiator, followed by reaction with the double bond of the ‘ene’ species (Figure 2B).²⁷ In general, the reaction proceeds well with any type of non-sterically hindered ‘ene’ functionality, but an ‘ene’ functionality that cannot undergo competitive chain-growth homo-polymerization (such as norbornenes and vinyl ethers)²⁷ is preferred. This also provides superior control over the reaction and concomitant homogeneity within the resulting network.²⁷ To obtain a thiol-ene photo-crosslinkable gelatin, it has to contain ‘ene’ functionalities (typically norbornene, vinyl esters or allyl ethers) which can be crosslinked using a multi-functional, thiolated crosslinker (e.g. dithiothreitol) (Figure 2C).^{1,22-24} Alternatively, gelatin can be functionalised with thiols and then crosslinked using a multi-functional ‘ene’ crosslinker (e.g. poly(ethylene glycol) diacrylate PEGDA).^{28,29}

Thiol-ene ‘photo-click’ hydrogels form more homogeneous networks with less shrinkage than chain-growth hydrogels due to the highly orthogonal nature of the reaction.³⁰ Additionally, they are not susceptible to oxygen inhibition and generally have faster reaction rates (e.g. gel-point for Gel-NB + DTT 2.7 s vs Gel-MOD 64.7 s).^{22,27,30} The reaction rate is highest when norbornene functionalities are used, due to their “spring-loaded” behavior that results from the ring strain relief upon reaction, as well as the rapid thiol-hydrogen abstraction rate by the carbon-centred radical.^{1,24,31} Furthermore, the percentage of reactive functional groups can be fully controlled by varying the thiol-ene ratio prior to crosslinking.^{22,27,30} In general, thiol-ene systems are more suitable for cell encapsulation than chain-growth systems, since the concentration of radical species is generally at least one order of magnitude lower than that of chain-growth hydrogel systems (where more radicals need to be formed to overcome oxygen inhibition).^{1,30,32} Drawbacks of the step-growth method include the necessity of an additional multi-functional, thiolated crosslinker in the reaction mixture, which cross-reacts with other thiols to form disulfides.²⁶ The probability of disulfide formation increases over time at elevated temperature (e.g. the half-life of DTT at pH 8.5 shifts from 11 h at 0°C to only 0.2 h at 40°C). This complicates the issue significantly, since higher temperatures are essential to maintain gelatin solubility during the bioprinting process.²⁵ Furthermore, step-growth hydrogels generally have significantly lower storage moduli than their chain-growth counterparts.^{1,22}

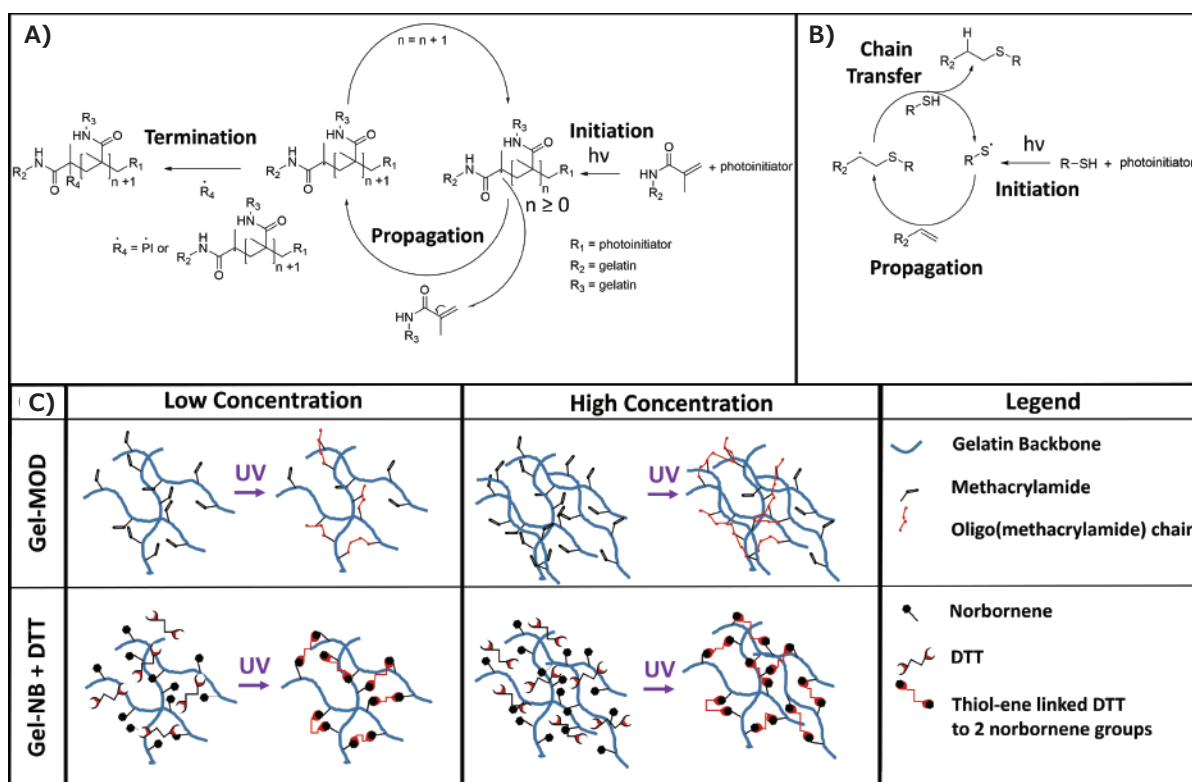


Figure 2. Illustration of chain-growth (Gel-MOD) v. is step-growth (Gel-NB + DTT) crosslinking using thiol-ene photoclick chemistry. Adapted with permission from reference 22, copyright 2018 Wiley.

Controlling Mechanical Properties of Photo-Crosslinkable Gelatins

The mechanical properties of photo-crosslinkable gelatin hydrogels can be tuned by adjusting various parameters of the gelatin itself or during material processing.

Influencing the Mechanical Properties by Chemical Modification

The number of crosslinkable functionalities has a large effect on the final mechanical properties of the material.^{4,5} For most derivatives, the number of reacted primary amines, and thus the degree of substitution, can be controlled by varying the molar ratio of the functionalizing reagent (e.g. methacrylic anhydride,⁴ carbic anhydride,¹ 5-norbornene-2-carboxylic acid²²) to match the number of primary amines present in the gelatin. When all primary amines are converted into crosslinkable functionalities, the mechanical properties can be increased even further by modifying the carboxylic acids in the side chains of aspartic acid and glutamic acid with additional crosslinkable functionalities such as 2-aminoethyl methacrylate.⁵ As a consequence, up to five times stiffer hydrogels can be obtained.⁵ Alternatively, the mechanical properties of gelatin-methacrylamide can be altered through covalent linking to a biopolymer such as alginate prior to crosslinking.³³ Although this resulted in a weaker hydrogel than pure gelatin-methacrylamide, the modification enabled fine control of the final mechanical properties through incorporation of divalent cations to physically crosslink the alginate chains.³³ In addition, the protein and polysaccharide chains formed a crosslinked network, resulting in a hydrogel that more accurately mimics the ECM in terms of chemical composition.³³

Influencing the Mechanical Properties During Hydrogel Processing

Once the crosslinked gelatin hydrogel has been synthesized, there are several ways to influence its mechanical properties during processing. For example, one approach is to co-crosslink it with another photo-crosslinkable material, which can be either natural (e.g. polysaccharide) or synthetic (e.g. PEG).^{1,34,35}

However, if a single material type is required, the mechanical properties of the final hydrogel can be influenced by varying the gelatin concentration in the hydrogel precursor solution. The higher the initial gelatin concentration, the stiffer the resulting hydrogels.^{4,5,21,22} However, evidence suggests that high gelatin concentrations (>15 w/v%) also negatively affect biocompatibility.²¹

Variation in the amount of irradiation applied during crosslinking can also affect the final mechanical properties of the material.^{5-7,21} Generally, lower doses result in lower crosslink densities and thus weaker hydrogels,^{7,21} but lower doses also yield more unreacted, potentially cytotoxic functionalities. Additionally, when chain-growth hydrogels are used, lower irradiation doses often reduce reproducibility due to the complex reaction kinetic profile and oxygen inhibition during crosslinking.²⁷ Furthermore, when using highly reactive thiol-ene systems, the influence of the dose is less apparent since the material can fully crosslink at very low doses, though there is a clear correlation between irradiation energy and swelling degree. For example, during two-photon polymerization, 20 mW irradiation at 100 mm/s results in a fully crosslinked network from 40 mW onwards when applied to gel-NB, but more than 80 mW is required to fully crosslink gel-MOD.^{5,22}

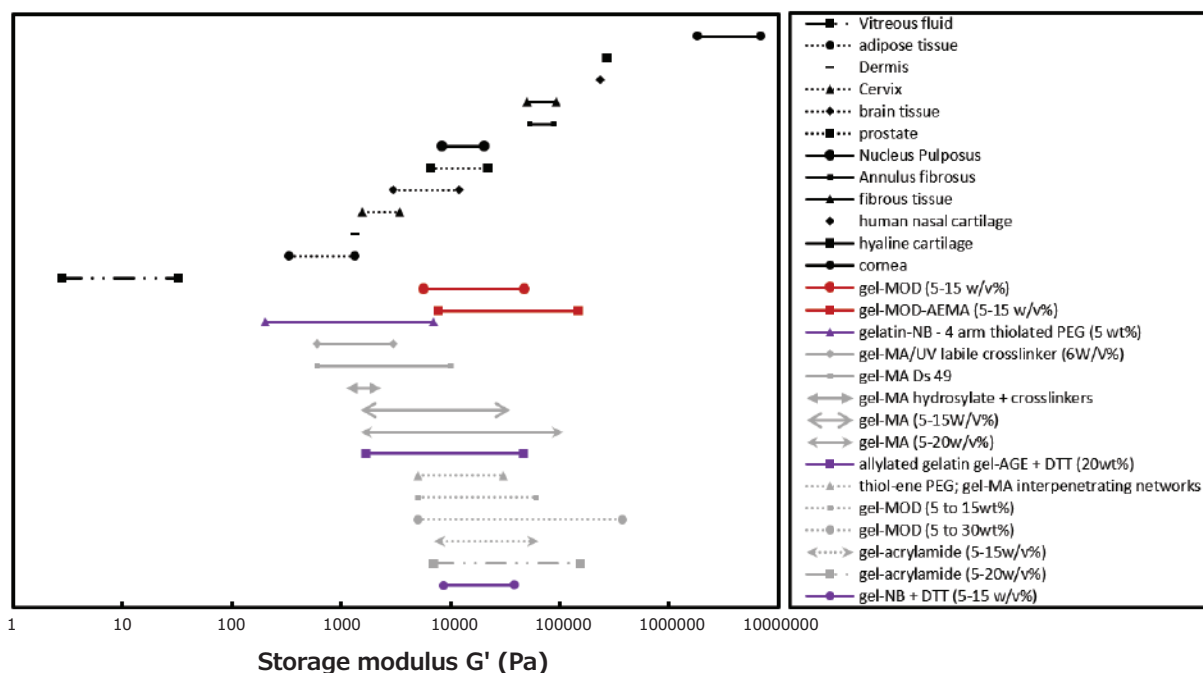


Figure 3. Scheme of the mechanical properties of different crosslinked gelatin hydrogels compared to the mechanical properties of various tissue types. Adapted with permission from reference 5, copyright 2017 ACS, with the inclusion of the mechanical properties of thiol-ene hydrogels from references 22 and 24. Hydrogels presented from the original reference are depicted in red, native tissues are depicted in black, chain-growth hydrogel systems are depicted in grey, and step-growth hydrogel systems are depicted in purple.)

When using thiol-ene hydrogel systems, additional control over the final mechanical properties is possible. Varying the thiol-ene ratio allows fine control over the number of reacted functionalities, as well as the mechanical properties of the final product.^{1,22,27} A higher number of reactive thiols per crosslinker molecule results in stiffer hydrogels, as the crosslink density increases.¹

This flexibility allows production of gelatin hydrogels suitable for a broad range of mechanical properties. A non-exhaustive overview of the mechanical range of gelatin derivatives compared to the mechanical properties of different tissues can be found in **Figure 3**.⁵ As a consequence, gelatin-based materials are extremely versatile tools for mimicking the mechanical properties of a plethora of tissues.

Gelatin Processing Via Additive Manufacturing

Gelatin hydrogels have been processed using a wide range of additive manufacturing techniques, including both direct methods, in which the material is applied directly in the additive manufacturing (AM) step,⁷ and indirect methods, where a template generated using AM is applied to control the shape of a secondary hydrogel material. Indirect approaches are usually applied to combine the mechanical properties of a stiff polymer with the desirable cell interactivity of gelatin, or to introduce complex 3D structures into materials which cannot be processed through a direct AM method.^{4,12,15,36}

Here, we focus on light-induced additive manufacturing techniques, more specifically, high-resolution additive manufacturing techniques such as two-photon polymerization (2PP), which is often referred to as direct laser writing. The technique uses the non-linear two-photon absorption to induce localized crosslinking, resulting in sub-micrometer spatial resolution. By tightly focussing a femtosecond laser beam into the material, conditions can be met for simultaneous interaction of two photons each possessing half the energy required to bridge the band gap required for photoinitiator excitation (**Figure 4A**), resulting in highly localized polymerization.^{5,37,38} Furthermore, since the probability of 2PP is only high in the very small voxel determined by the applied optics and laser power, the polymerisation is confined to a 3D volume element often smaller than the expected diffraction limit. This is in contrast to conventional light-based additive manufacturing techniques using single photon (i.e. linear) absorption, where polymerization can occur throughout the entire beam path and is only limited by its penetration depth.^{5,39}

As a consequence, structures with subcellular dimensions can be produced with 2PP, making it suitable for studying more complex cell-biomaterial interactions. In 2011, we were the first to report the generation of gelatin-based tissue engineering scaffolds using primary adipose tissue-derived stem cells using this method.¹⁴

Since then, multiple studies have been reported dealing with 2PP processing of modified gelatins, most of them using gelatin-methacrylamide (Gel-MOD).^{23,40,41} Using this gelatin derivative, the successful use of 2PP was even reported in the presence

of living cells.¹³ Although the cells did not survive direct exposure to the laser during structuring, it was possible to use 2PP to entrap cells within 3D microstructures (**Figure 4B**).¹³ Furthermore, cytotoxicity was not due to spatiotemporal irradiation by the laser or the photo-initiator, but instead could be attributed to formation of cytotoxic species within the cells as a side-product of photo-initiator activation.¹³ This hypothesis was later substantiated with a macromolecular photo-initiator based on hyaluronic acid, which enabled 2PP processing combined with the encapsulation of living cells, even within the exposed areas (**Figure 4C**).⁴² The study indicated that the previously observed cytotoxicity originated from the penetration of the low molecular weight photo-initiator through the cell membrane, thereby resulting in photo-oxidative damage within the cell during irradiation. By immobilizing the photo-initiator onto a macromolecule, cell barrier penetration was prevented, thereby allowing 2PP in the presence of living cells.⁴²

Despite these successful approaches, gelatin-methacrylamide does have some limitations for 2PP processing. In general, due to poor reaction kinetics and associated mechanical properties, relatively high gelatin concentrations (>15 wt%) and light dose (eg. 330 mW at 7 mm/s scan speed) are required to crosslink the material.^{13,14,40,43} Most importantly, subsequent swelling of the 2PP-produced structures can negate the high-resolution capacity of this approach.

Other strategies involve the application of a secondary material to function as a mechanical support,^{35,43} either by indirect additive manufacturing (discussed below), or by first structuring a stronger material to function as support, such as a mixture of hydrophobic acrylates, followed by subsequent gelatin crosslinking.⁴¹ Alternatively, a secondary material such as poly(ethylene glycol) diacrylate (PEGDA) can be used for the formation of a co-network, thereby benefitting from the higher mechanical properties of PEG, along with superior acrylate-based reaction kinetics.³⁵

To overcome these limitations, we have developed a gelatin derivative in which all primary amines were converted to methacrylamides (0.385 mmol/g gelatin), while additional methacrylates were introduced onto the carboxylic acids. This resulted in 1 mmol of crosslinkable groups per gram of gelatin (**Figure 1C**).⁵ As a consequence, a denser gelatin network was formed, exhibiting both higher stiffness and with little to no post-production swelling. Additionally, the reaction kinetics were improved compared to conventional gelatin-methacrylamide, thereby resulting in a broader 2PP spatiotemporal processing range (**Figure 1A**).⁵ Furthermore, 2D experiments indicated a comparable biocompatibility with both fibroblasts (L929) and osteoblasts (MC3T3) for Gel-MOD-AEMA and the well-established Gel-MOD.⁵

Although the introduction of these additional functionalities drastically improved 2PP processing, the crosslinking reactions remained subject to the drawbacks associated with chain-growth hydrogels discussed earlier. To further improve the material processing range, 2PP experiments were explored using thiol-ene photoclick hydrogels.^{22,23} In order to maximally exploit the

improved reactivity of thiol-ene hydrogel systems, gelatin type B was modified to include norbornene functionalities. Gel-NB was then processed via 2PP using DTT as the thiolated crosslinker, resulting in a drastically improved spatiotemporal 2PP processing range compared to all previously reported gelatin derivatives. Only half of the energy was required to yield reproducible crosslinking (i.e. 20 mW at 100 mm/s for Gel-NB DS 63 vs 40 mW at 100 mm/s for Gel-MOD-AEMA) despite a four times lower concentration of crosslinkable functionalities (i.e. 0.24 mmol/g for Gel-NB vs 1 mmol/g for Gel-MOD-AEMA). Additionally, increasing the laser power above 40 mW did not influence the hydrogel swelling behaviour, which indicated that the material was already fully crosslinked. This is in contrast to Gel-MOD-AEMA, for which an increase of the laser power resulted in a concomitant decrease in swelling ratios.^{5,22} Furthermore, a

broader concentration range could be applied for 2PP processing with Gel-NB, since reproducible structuring was reported for the first time below 10 w/v% gelatin concentration (i.e. 5w/v%).²² It should be noted, that Gel-NB has a significantly lower swelling ratio than Gel-MOD, due to the hydrophobic nature of the norbornene functionalities.²² As a consequence, a better computer-aided design/computer-aided manufacturing (CAD/CAM) mimicry is observed with Gel-NB, while the lower spatiotemporal energy required for full conversion leads to stiffer gels at lower laser powers. This enables the use of gel-NB for the fabrication of complex structures able to support their own weight, despite the presence of only small supporting structures (Figure 4D and E). In addition, the material can be used for the fabrication of micro-scaffolds which were fully populated by fibroblasts after 7 days of culture (Figure 4D).²²

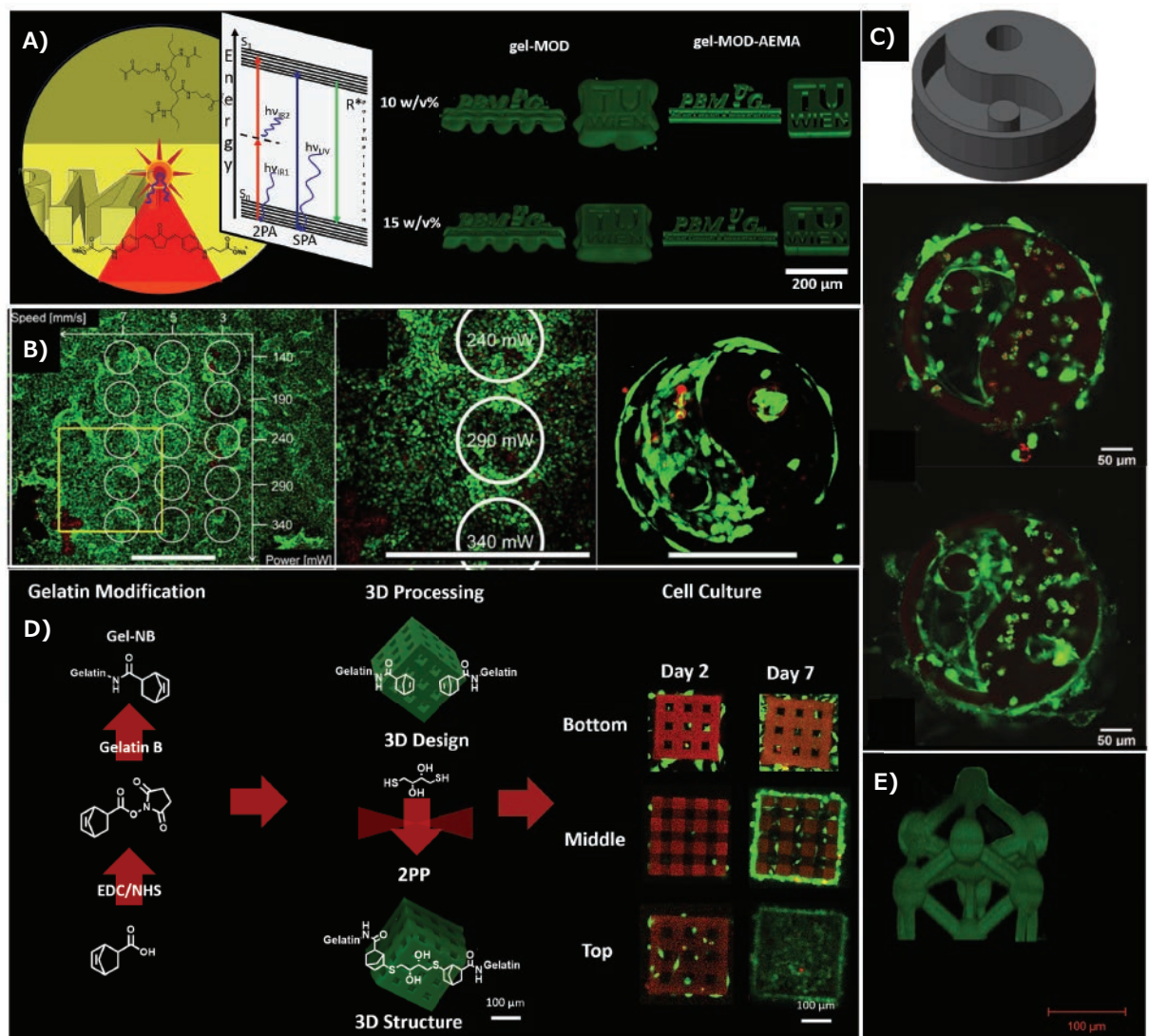


Figure 4. A) Comparison between two-photon and single-photon polymerization principle including a Jablonski diagram; Difference in shape fidelity between Gel-MOD and Gel-MOD-AEMA due to post-production swelling. Adapted with permission from reference 5, copyright 2017 ACS. B) Influence of different laser powers and scan speeds on cell viability (left and center panel, scale bars represent 1 mm). 3D structure with encapsulated MG 63 cells after 3 weeks cell culture (right panel, scale bar represents 200 μ m). Adapted with permission from reference 13, copyright 2014 ACS. C) CAD image (top) of structure produced inside Gel-MOD using the macromolecular two-photon photoinitiator in the presence of MC3T3 cells (center and bottom panel). Reproduced with permission from reference 42, copyright 2017 Royal Society of Chemistry. D) Scheme demonstrating the modification of gelatin into Gel-NB, 2PP structuring following a thiol-ene photoclick reaction into a microstructure, subsequent cell culture in the presence of L929 fibroblasts after 2 and 7 days of cell culture. Reproduced with permission from reference 22, copyright 2018 Wiley. E) Atomium microstructure generated via 2PP in a 10 w/v% Gel-NB - DTT solution with an equimolar thiol/ene ratio. Image courtesy of MSc. J. Van Hoorick.

Conclusions

Throughout the past two decades, a plethora of photo-crosslinkable gelatins suitable for tissue engineering purposes have emerged. The successful biofabrication strategies, in combination with desirable biocompatibility, cell interactivity and cost-effectiveness, have resulted in the commercialization of several photo-crosslinkable gelatin derivatives. Due to recent success with thiol-ene based systems, commercialisation of these derivatives is also anticipated soon. In addition, the combination of the availability of off-the-shelf materials, declining costs, and improved additive manufacturing technologies is likely to produce high-end biofabrication breakthroughs and subsequent integration in a clinical setting. Since gelatin is already an FDA-approved material with widespread applications in the food and pharmaceutical industry, it is only a matter of time until biofabrication strategies using photo-crosslinkable gelatins will be commonplace in the clinic.

Acknowledgement

Jasper Van Hoorick was granted an FWO-SB PhD grant provided by the Research Foundation Flanders (FWO, Belgium). The FWO-FWF grant (a bilateral Research Foundation Flanders — Austrian Science Fund project) is acknowledged for financial support.

References

- Münz, Z.; Shih, H.; Lin, C.-C. *Biomater. Sci.* **2014**, *2*, 1063.
- Rose, J. B.; Pacelli, S.; El Haj, A. J.; Dua, H. S.; Hopkinson, A.; White, L. J.; Rose, F. R. *J. Materials (Basel)* **2014**, *7*, 3106.
- "Gelatin, Report No. 58," <http://wayback.archive-it.org/7993/20171031062708/https://www.fda.gov/Food/IngredientsPackagingLabeling/GRAS/SCOGS/ucm261307.htm>, **1979**.
- Van Hoorick, J.; Declercq, H.; De Muynck, A.; Houben, A.; Van Hoorebeke, L.; Cornelissen, R.; Van Erps, J.; Thienpont, H.; Dubruel, P.; Van Vlierberghe, S. *J. Mater. Sci. Mater. Med.* **2015**, *26*, 247.
- Van Hoorick, J.; Gruber, P.; Markovic, M.; Tromayer, M.; Van Erps, J.; Thienpont, H.; Liska, R.; Ovsianikov, A.; Dubruel, P.; Van Vlierberghe, S. *Biomacromolecules* **2017**, DOI 10.1021/acs.biomac.7b00905.
- Van Den Bulcke, A. I.; Bogdanov, B.; De Rooze, N.; Schacht, E. H.; Cornelissen, M.; Berghmans, H. *Biomacromolecules* **2000**, *1*, 31.
- Billiet, T.; Gevaert, E.; De Schryver, T.; Cornelissen, M.; Dubruel, P. *Biomaterials* **2014**, *35*, 49.
- Van Vlierberghe, S. *J. Mater. Sci.* **2016**, *51*, 1.
- Bigi, A.; Cojazzi, G.; Panzavolta, S.; Rubini, K.; Roveri, N. *Biomaterials* **2001**, *22*, 763.
- Schacht, E. H.; Van Den Bulcke, A. I.; Delaey, B.; Draye, J.-P. *Medicaments Based on Polymers Composed of Methacrylamide-Modified Gelatin*, **2002**, US 6458386 B1.
- Klotz, B. J.; Gawlitta, D.; Rosenberg, A. J. W. P.; Malda, J.; Melchels, F. P. W. *Trends Biotechnol.* **2016**, *34*, 394.
- Markovic, M.; Van Hoorick, J.; Hözl, K.; Tromayer, M.; Gruber, P.; Nürnberger, S.; Dubruel, P.; Van Vlierberghe, S.; Liska, R.; Ovsianikov, A. *J. Nanotechnol. Eng. Med.* **2015**, *6*, 210011.
- Ovsianikov, A.; Mühleder, S.; Torgersen, J.; Li, Z.; Qin, X.-H.; Van Vlierberghe, S.; Dubruel, P.; Holthoner, W.; Redl, H.; Liska, R.; Stampf, J. *Langmuir* **2014**, *30*, 3787.
- Ovsianikov, A.; Deiwick, A.; Van Vlierberghe, S.; Pflaum, M.; Wilhelmi, M.; Dubruel, P.; Chichkov, B. *Materials (Basel)* **2011**, *4*, 288.
- Van Rie, J.; Declercq, H.; Van Hoorick, J.; Dierick, M.; Van Hoorebeke, L.; Cornelissen, R.; Thienpont, H.; Dubruel, P.; Van Vlierberghe, S.; *J. Mater. Sci. Mater. Med.* **2015**, *26*, 5465.
- Loessner, D.; Meinert, C.; Kaemmerer, E.; Martine, L. C.; Yue, K.; Levett, P. A.; Klein, T. J.; Melchels, F. P. W.; Khademhosseini, A.; Huttmacher, D. W. *Nat. Protoc.* **2016**, *11*, 727.
- Yue, K.; Trujillo-de Santiago, G.; Alvarez, M. M.; Tamayol, A.; Annabi, N.; Khademhosseini, A. *Biomaterials* **2015**, *73*, 254.
- Hözl, K.; Lin, S.; Tytgat, L.; Van Vlierberghe, S.; Gu, L.; Ovsianikov, A. *Biofabrication* **2016**, *8*, 32002.
- "Allevi3D," can be found under <https://allevi3d.com/shop/>, n.d.
- "Merck," can be found under <https://www.sigmaaldrich.com/catalog/substance/gelatinmethacryloyl1234598765?lang=en®ion=BE>, n.d.
- Billiet, T.; Van Gasse, B.; Gevaert, E.; Cornelissen, M.; Martins, J. C.; Dubruel, P. *Macromol. Biosci.* **2013**, *13*, 1531.
- Van Hoorick, J.; Gruber, P.; Markovic, M.; Rollot, M.; Graulus, G.; Vagenende, M.; Tromayer, M.; Van Erps, J.; Thienpont, H.; Martins, J. C.; Baudis, S.; Ovsianikov, A.; Dubruel, P.; Van Vlierberghe, S. *Macromol. Rapid Commun.* **2018**, *39*(14), e1800181.
- Qin, X.-H.; Torgersen, J.; Saf, R.; Mühleder, S.; Pucher, N.; Ligon, S. C.; Holthoner, W.; Redl, H.; Ovsianikov, A.; Stampf, J.; Liska, R. *J. Polym. Sci. Polym. Chem.* **2013**, *51*, 4799.
- Bertlein, S.; Brown, G.; Lim, K. S.; Jungst, T.; Boeck, T.; Blunk, T.; Tessmar, J.; Hooper, G. J.; Woodfield, T. B. F.; Groll, J. *Adv. Mater.* **2017**, *29*, 1703404.
- Stevens, R.; Stevens, L.; Price, N. C. in *Biochem. Educ.* **11**, **1983**, 70.
- Pereira, R. F.; Bártolo, P. *J. Engineering* **2015**, *1*, 90.
- Hoyle, C. E.; Bowman, C. N. *Angew. Chemie* **2010**, *49*, 1540.
- Van Vlierberghe, S.; Schacht, E.; Dubruel, P. *Eur. Polym. J.* **2011**, *47*, 1039.
- Xu, K.; Fu, Y.; Chung, W.; Zheng, X.; Cui, Y.; Hsu, I. C.; Kao, W. J. *Acta Biomater.* **2012**, *8*, 2504.
- Lin, C.-C.; Ki, C. S.; Shih, H. *J. Appl. Polym. Sci.* **2015**, *132*, 1.
- Hoyle, C. E.; Lee, T. A. I. Y.; Roper, T. J. *Polym. Sci. Part A Polym. Chem.* **2004**, *42*, 5301.
- Mccall, J. D.; Anseth, K. S. *Biomacromolecules* **2012**, *13* (8), 2410.
- Graulus, G.-J.; Mignon, A.; Van Vlierberghe, S.; Declercq, H.; Fehér, K.; Cornelissen, M.; Martins, J. C.; Dubruel, P. *Eur. Polym. J.* **2015**, *72*, 494.
- Tytgat, L.; Vagenende, M.; Declercq, H.; Martins, J. C.; Thienpont, H.; Ottevaere, H. *Carbohydr. Polym.* **2018**, *189*, 1.
- Brigo, L.; Urciuolo, A.; Giulitti, S.; Della, G.; Tromayer, M.; Liska, R.; Elvassore, N.; Brusatin, G. *Acta Biomater.* **2017**, *55*, 373.
- Houben, A.; Van Hoorick, J.; Van Erps, J.; Thienpont, H.; Van Vlierberghe, S.; Dubruel, P. *Ann. Biomed. Eng.* **2016**, *45*, 58.
- Van Hoorick, J.; Ottevaere, H.; Thienpont, H.; Dubruel, P. *Polymer and Photonic Materials Towards Biomedical Breakthroughs*, **2018**.
- Qin, X.-H.; Ovsianikov, A.; Stampf, J.; Liska, R. *BioNanoMaterials* **2014**, *15*, 49.
- Ovsianikov, A.; Mironov, V.; Stampf, J.; Liska, R. *Expert Rev. Med. Devices* **2012**, *9*, 613.
- Ovsianikov, A.; Deiwick, A.; Van Vlierberghe, S.; Dubruel, P.; Lena, M.; Dräger, G.; Chichkov, B. *Biomacromolecules* **2011**, *12*, 851.
- Engelhardt, S.; Hoch, E.; Borchers, K.; Meyer, W.; Krüger, H.; Tovar, G. E. M.; Gillner, A. *Biofabrication* **2011**, *3*, 25003.
- Tromayer, M.; Gruber, P.; Markovic, M.; Rosspaintner, A.; Vauthey, E.; Redl, H.; Ovsianikov, A.; Liska, R. *Polym. Chem.* **2017**, *8*, 451.
- Engelhardt, S.; Hoch, E.; Borchers, K.; Meyer, W.; Krüger, H.; Tovar, G. E. M.; Gillner, A. *Biofabrication* **2011**, *3*, 25003.

Gelatin

Name/Type	Gel Strength (Bloom)	H ₂ O (mg/mL)	Cat. No.
Gelatin from porcine skin Type A	300	soluble 50	G2500-100G G2500-500G G2500-1KG
	90-110	-	G6144-100G G6144-500G G6144-1KG
	300	-	G1890-100G G1890-500G G1890-1KG
	175	soluble 50	G2625-100G G2625-500G G2625-1KG

Functionalized Gelatin

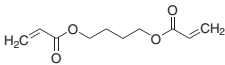
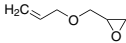
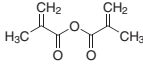
Allyl-Modified Gelatin

Name	Gel Strength (Bloom)	Degree Of Functionalization	Cat. No.
Allyl-modified gelatin	300	70% by TNBS method	901553-1G

Gelatin Methacryloyl

Name	Gel Strength (Bloom)	Degree Of Functionalization	Cat. No.
Gelatin methacryloyl	300	80%	900496-1G
	300	60%	900622-1G
	300	40%	900629-1G
	90-110	60%	900628-1G
	170-195	60%	900741-1G

Building Blocks for Gelatin Functionalization

Name	Structure	Purity	Cat. No.
1,4-Butanediol diacrylate		90%	411744-25ML 411744-100ML 411744-1L
5-Norbornene-2-carboxylic acid, mixture of <i>endo</i> and <i>exo</i> , predominantly <i>endo</i>		98%	446440-25ML
Allyl glycidyl ether		≥99%	A32608-100ML A32608-500ML
<i>cis</i> -5-Norbornene- <i>endo</i> -2,3-dicarboxylic anhydride		99%	247634-5G 247634-25G
Methacrylic anhydride		94%	276685-100ML 276685-500ML

subscribe today

Don't miss another topically focused technical review.

It's **free** to sign up for a print or digital subscription of *Material Matters*™.

- Advances in cutting-edge materials
- Technical reviews on emerging technology from leading scientists
- Peer-recommended materials with application notes
- Product and service recommendations



To view the library of past issues or to subscribe, visit

SigmaAldrich.com/materialmatters

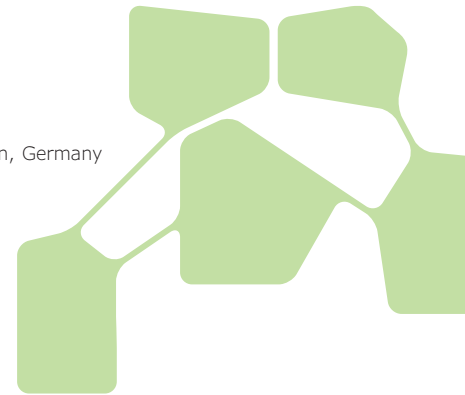
**MILLIPORE
SIGMA**

Controlled Fabrication Methods for Tissue Engineering Constructs



David B. Gehlen and Laura De Laporte*

DWI – Leibniz-Institute for Interactive Materials, Aachen, Germany
*Email: delaporte@dwi.rwth-aachen.de



Introduction

Organ failure is a major health issue that affects millions of patients annually and costs hundreds of billions US dollars. For the last 30 years, scientists have been combining the tools, methods, and molecules from engineering, biology, chemistry, and physics in order to fabricate new tissues for the restoration or replacement of damaged organs with functional ones.¹ This field, known as tissue engineering, has three main subfields: i) *ex vivo* generation of implantable tissue using material scaffolds with cells and growth factors, ii) biohybrid materials with or without cells to trigger regeneration *in vivo*, and iii) *ex vivo* tissue models to study tissue formation and pathological processes in combination with drugs (Figure 1).

Material Selection To Build Tissue Constructs

Over the last few decades, researchers have developed two major paths for the growth of tissue constructs in different sizes and complexities: implantable scaffolds and injectable hydrogels. Scaffolds for implantation or *ex vivo* tissue models

can be built with intricate architectures since the materials are processed outside the body. For example, one technique is decellularization of natural tissues to create structures very similar to the original (Figure 2A). In the first animal experiment in 1995, decellularized small intestinal submucosa from pigs were implanted in dogs, resulting in improved Achille’s tendon repair. In 2010, a decellularized trachea was successfully implanted in a 10-year-old child. In initial experiments, tissue was decellularized by immersing it in a detergent solution. More recent methods use the native vascular network for perfusion and recellularization,² allowing for the creation of whole liver and other types of grafts.³ Even though decellularization techniques have improved significantly and now maintain most of the essential extracellular matrix (ECM) components, many challenges remain. These include inflammatory responses, better preservation of the biochemical and physical integrity of the entire ECM and optimized bioreactors for efficient recellularization.

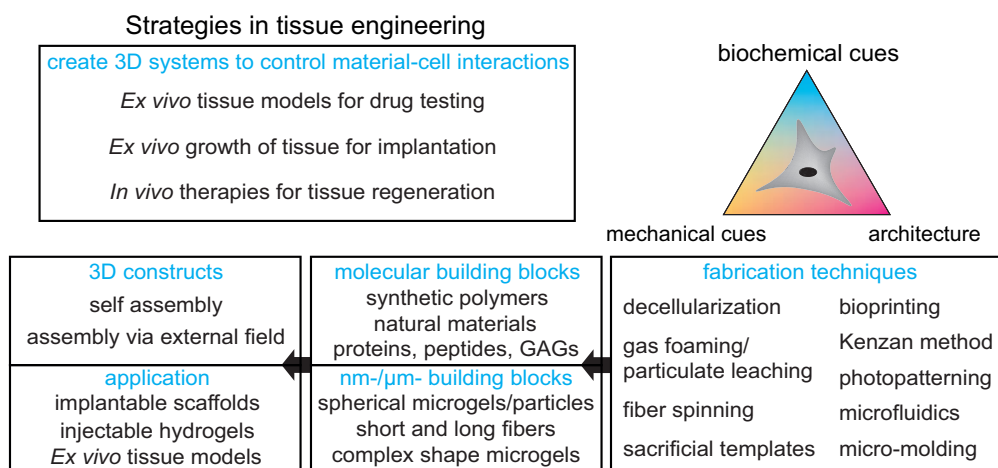


Figure 1. Strategies for designing biomaterial constructs: Different fabrication techniques can be used to combine molecular and nano and micrometer size building blocks to form 3D matrices for implantable scaffolds, injectable applications, or *ex vivo* tissue models.

To study material/cell interactions in a systematic way, scientists are building constructs using both natural and synthetic materials, two components with important differences. While natural materials, such as collagen, fibrin, and Matrigel® inherently contain many biological signals, artificial synthetic ECMs (aECM) are prepared with a small number of well-defined building blocks. To form functional tissue, these matrices mimic the mechanical, biochemical, and structural properties of the ECM, including degradability. In order to incorporate cells during preparation, physiological conditions and biocompatible chemistry must be maintained. Nowadays, most materials are biohybrid systems that combine the controllability of synthetic materials with the biological activity of natural compounds.

Fabrication Methods for Solid Implantable Scaffolds

The material properties have to be designed at multiple scales, from the physical, chemical, and biochemical properties of the molecules to the nano and micrometer scale of the porosity and structural elements, all the way up to the macroscopic architecture. Solvent casting is one of the earliest methods used for the preparation of implantable scaffolds, where a polymer is dissolved in an evaporating organic solvent using leachable

porogens such as salt particles.⁴ However, the cytotoxicity of organic solvents made it impossible to add cells or proteins during preparation. Subsequently, more biocompatible methods such as freeze-drying and gas foaming particulate leaching have been developed that enable both the incorporation of bioactive molecules and the creation of more complex architectures. For example, constructs with aligned channels can be fabricated to mimic oriented tissues, such as the spinal cord (**Figure 2B**). Another method is fiber spinning, which allows the creation of fibrous mats with random or oriented fibers in which the diameter, fiber density, and topography can be controlled. The most popular spinning method is electrospinning, where electrostatic forces induce a Taylor cone, accelerating the solution towards a collector with the opposite polarity, producing synthetic fibers as the solvent evaporates (**Figure 2C**).⁵ The first electrospun mats for tissue engineering were used as a vascular prosthesis in 1978. Another method, solvent-assisted spinning, does not apply an electric field, but the fibers are mechanically pulled and collected by a rotating drum. This enables the formation of fibers with larger diameters and more controllable inter-fiber distances, fiber orientation, and fiber topography. In wet spinning, polymers are dissolved in a non-volatile solvent and extruded inside a solution, which washes the solvent out,

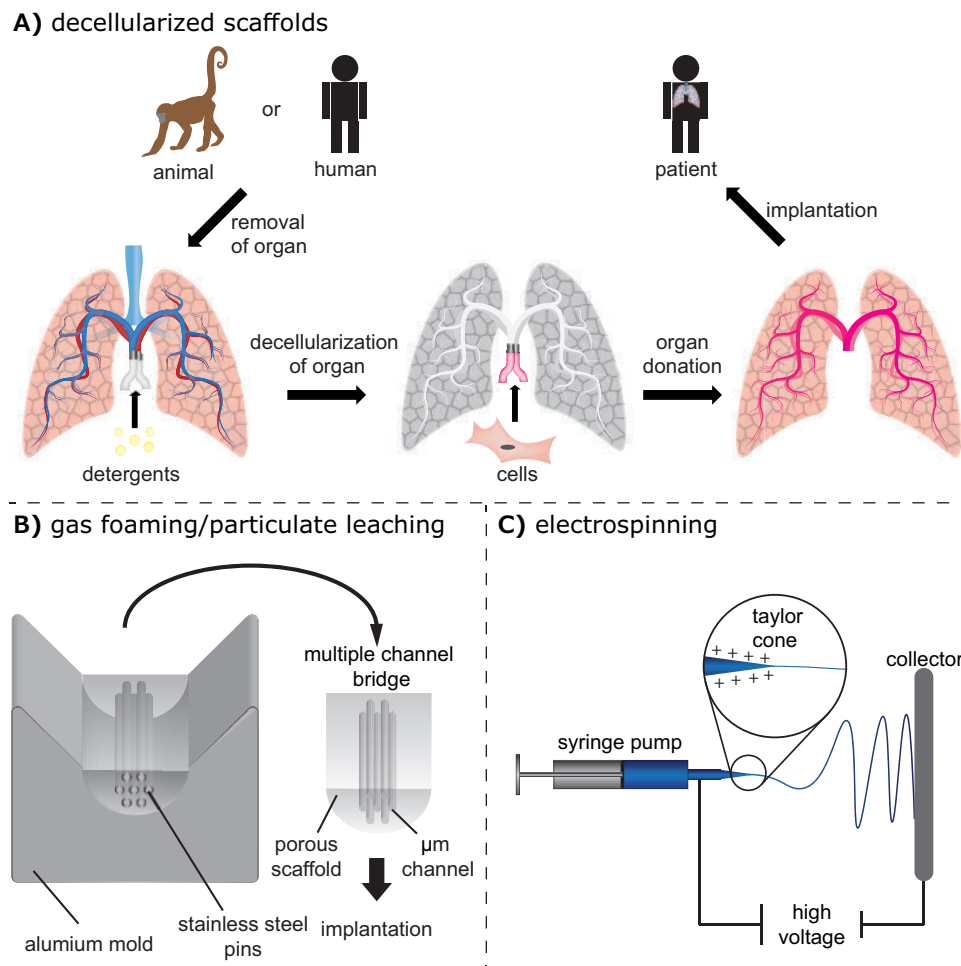


Figure 2. A) Decellularization of tissues and subsequent recellularization for the production of vascularized tissue engineered constructs for potential implantation. B) Production of multiple channel spinal cord bridges using a gas foaming/particulate leaching technique. C) Electrospinning of nano and micrometer sized fibers for implantable scaffolds.

resulting in rapid fiber production. Thermo-stable polymers can be molten without using a solvent and pressed out of a nozzle during melt-spinning, then cooled by air flow between the nozzle and the collector. This technique has the advantage of not requiring further washing steps.

Fabrication Methods for Hydrogel-based Scaffolds

The previously mentioned fabrication methods create solid implantable scaffolds but natural tissues are often softer and viscoelastic. Hydrogels are water-containing networks that mimic these properties, and are prepared by crosslinking hydrophilic natural or synthetic proteins, polymers, or sugars. Crosslinks are achieved through physical interactions and reversible bonds, and/or by chemical reactions and covalent bonds, triggered for example, by ionic interactions, pH, temperature, or enzymes.⁶ Fully synthetic polymers, glycosaminoglycans (GAGs), and recombinant proteins are used to prepare hydrogels with minimized batch-to-batch variability that avoid potential pathogenic contaminations. In order to create hydrogels, building blocks such as poly(ethylene glycol) (PEG) or polyacrylamide, bioactive peptides, ECM fragments, and proteins are coupled or mixed within the network. If the ability to induce degradation is desired, the linkers between the molecules or the molecules themselves can be designed with ester bonds amenable to hydrolysis, or with matrix metalloproteinase (MMP)-sensitive cleavage sites. Combining an understanding of biocompatible chemical reactions, biochemistry, and physical chemistry, a large toolbox of hydrogels with different mechanical and biological properties has been established for a wide variety of applications.

The remaining challenge is to decouple the effects of different parameters, such as the pore size and distribution, stiffness, degradation rate, ligand spacing, and topography, on cell behavior. Another limitation is that most conventional hydrogels

have nano-size meshes, which prevent cell migration in the case of covalent and non-degradable crosslinks. When cells are mixed inside the hydrogels, either matrix degradation or reversible crosslinks are required to enable the cells to spread and migrate. Therefore, hydrogels with dynamic bonds have recently been designed and studied to better mimic the viscoelastic, strain-stiffening, and fibrous properties of the native ECM. To further improve infiltration of endogenous cells *in vivo* (which is challenging as cells choose the least resistant path around the hydrogel), macroporous hydrogels have been produced. Here, strategies differ for implants and injectable materials. For implants, sacrificial porogens or templates can create hydrogels with macroscopic pores and potentially shape-recovering properties (**Figure 3A**),⁷ but may not allow for simultaneous cell encapsulation into the hydrogel.

To address this problem, bioprinting has emerged as a way to print 3D hydrogel constructs in combination with cells and proteins. There are three methods of bioprinting: inkjet printing, micro-extrusion, and laser-assisted printing (**Figure 3 B–D**).⁸ While inkjet printing is a cheap and accessible method that deposits the material droplet-wise, micro-extrusion prints continuous lines and patterns, allowing for higher viscosities and cell densities. However, extrusion is slower, and maintaining cell viability is challenging due to high shear stresses. In the case of laser-assisted bioprinting, a focused, pulsed laser shoots micro-beats from a ribbon onto specific positions on a receiving substrate. This technology is more complex, elaborate, and costly, and requires fine-tuning for each application and cell type. However, it operates over a large range of viscosities and high cell densities, and cells remain viable during the process. While exceptional progress has been made in these printing techniques, a new generation of bioinks is needed to mimic the ECM properties without sacrificing printability in the presence of cells. The ideal bioink would be a non-cytotoxic liquid, that crosslinks

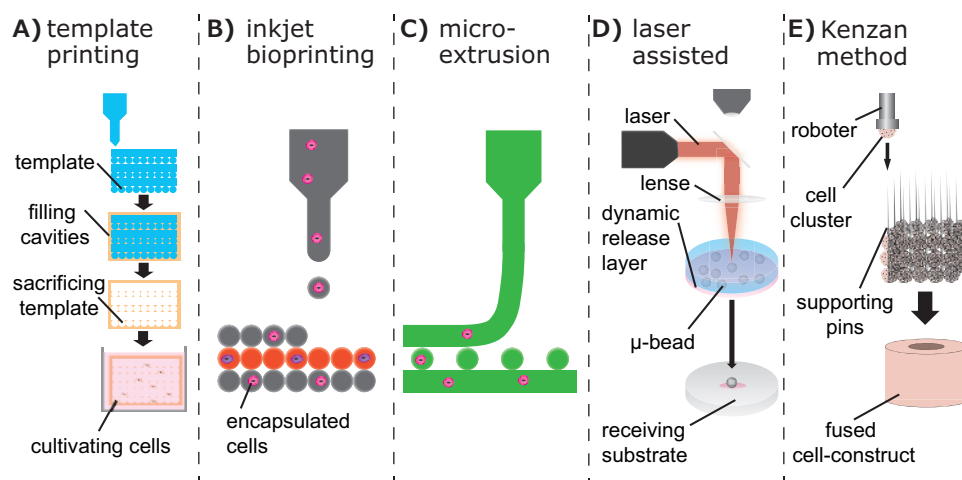


Figure 3. A) Sacrificial templates to create macroporous hydrogels. B) Droplet-wise inkjet bioprinting. C) Continuous line printing using micro-extrusion. D) Laser-assisted bioprinting using focused pulsed laser to shoot micro-beats on a receiving substrate. E) Kengan method to print cell spheroids directly without using supporting hydrogel-scaffolds.

only on demand (to prevent clogging of the nozzle), enables high cell densities without subjecting the cells to thermal and mechanical stress. The crosslinking trigger must not damage the cells and the crosslinking kinetics must be controllable and rapid enough to achieve high resolution. The resulting hydrogel has to be cell-adhesive and degradable with a tunable stiffness. As an alternative to bioink, the Kengan method prints cell spheroids directly without using a supporting hydrogel-scaffold (**Figure 3E**). Here, cell spheroids are robotically placed on micro-needles to achieve a specific structure — for example vascular tubes after fusion of the spheroids.⁹

As previously mentioned, hydrogel precursor solutions can be injected as a liquid and then crosslink *in situ* under physiological conditions using a minimally invasive procedure. This enables adaptation to irregular shapes inside the body, and forms a close interface with surrounding tissue provided that the crosslinking mechanism is fully optimized — fast enough to avoid leakage but slow enough to allow handling and precise injection. There are two major shortcomings with this method: i) the lack of macroscopic pores to facilitate infiltration of endogenous cells and ii) the formation of hierarchical and oriented structures to direct cell growth.

One approach to overcoming the first problem is to inject pre-crosslinked microgels, containing reactive groups that link together via a secondary crosslinking mechanism after injection. Macroscopic pores of various sizes can be created depending on the diameter of spherical microgels. These structures are called interconnected microporous annealed particle scaffolds (MAPs), and they significantly enhance cell infiltration and tissue healing compared to conventional hydrogels with the same polymer composition (**Figure 4A**).¹⁰ Microgels for this purpose are prepared via microfluidics using different materials, such as PEG or alginate, and linked together either covalently by enzymatic reactions or via specific interactions.¹¹ To obtain shear-thinning properties inside these MAPs, microgels are crosslinked using guest-host chemistry, enabling this material to be used as a bioink.¹² An alternative method for obtaining larger pores is

the creation of ECM-like fibrous structures via self-assembly of highly defined molecules using supramolecular chemistry. The pore size and strain-stiffening properties of the structure vary depending on the properties and lengths of the molecular building blocks (**Figure 4B**).¹³ These microporous structures have the advantage that cells do only interact with the aECM, but also with each other. These cell-cell interactions are crucial for many biochemical processes, including cell organization and maturation. For example, the stemness of neural progenitor cells in the absence of differentiation factors is highly dependent on the degradation rate and mechanism of the hydrogel, and thus on the ability of the cells to remodel the matrix over time and exert cadherin-mediated cell-cell interactions.¹⁴ Furthermore, during the development of the mesenchyme, cells initially exhibit significant interactions with the ECM, but over time they start to interact more with each other via cell-cell interactions, a process that is not yet completely understood.¹⁵

The second problem is the often isotropic character of injectable hydrogels. To induce hierarchy and orientation into these hydrogels, many different technologies are being developed, including photopatterning, orientation of self-assembling nanofibers, and the formation of guiding structures using an external magnetic field. Photopatterning uses light to create high-resolution structures of biochemical and/or mechanical patterns inside a hydrogel that can act as guiding cues. In this technique, a focused laser beam activates photosensitive molecules, resulting in local crosslinking and thus stiffening, degradation, exposure of functional groups, or post-modifications (**Figure 5A**).¹⁶ Two-photon lithography can achieve better resolution in the z-direction but, except for laser ablation, only relatively thin hydrogel layers of several millimeters can be photopatterned, so the fabrication of larger tissues, like heart or liver are currently not possible using this method. In the case of self-assembly, peptide amphiphiles turn into high aspect ratio nanofibers, which can be aligned over a centimeter range by manually dragging the fibrous structure into salty media (**Figure 5B**). These supramolecular filaments can be functionalized with bioactive peptides and support

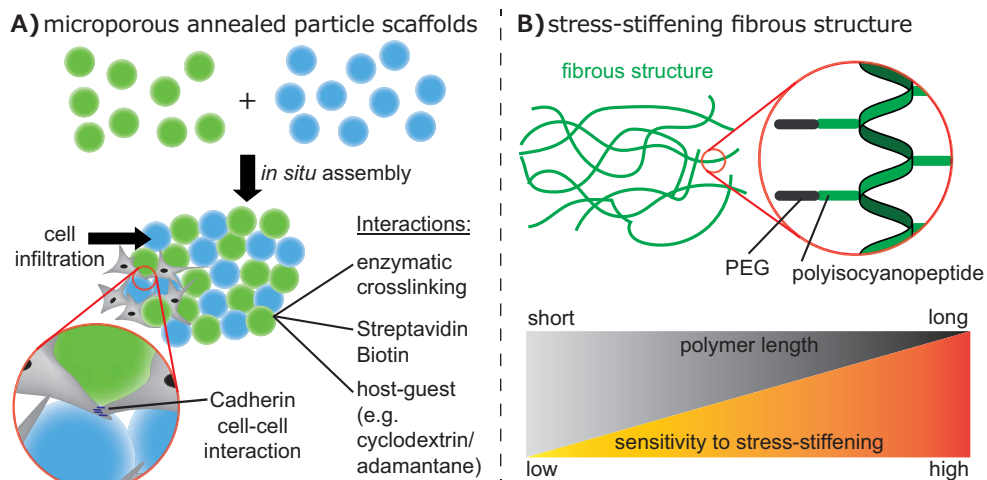


Figure 4. A) Assembly of spherical microgels using different interactions to promote cell infiltration into the scaffold and cell-cell interactions. B) Stress-stiffening fibrous structures using polyisocyanopeptides. Different polymer lengths can be used to control the stress-stiffening properties.

aligned neuronal cell growth.¹⁷ Even though this technique allows for a minimally invasive *in vivo* application, variation of the nanofiber dimensions is limited, and the alignment of the filaments depends on the direction of the flow inside the needle. As an alternative, magnetic fields can be applied to form strings of magnetic particles inside hydrogels (Figure 5C). These strings then function as guiding elements to orient cells, but their shapes and dimensions are difficult to control and a high concentration of cytotoxic iron oxide particles is required.

In the interest of obtaining more control of the anisotropy of injectable hydrogels with a minimal amount of iron oxide, the Anisogel (Anisotropic hydrogel) concept was developed. Anisogel is a hybrid hydrogel that consists of two components: magneto-responsive, micron-scale, rod-shaped guiding elements and a precursor solution. After injection, the guiding elements orient in the presence of an external magnetic field in the millitesla range within one minute, while the surrounding precursor solution crosslinks to fix the alignment of the oriented elements

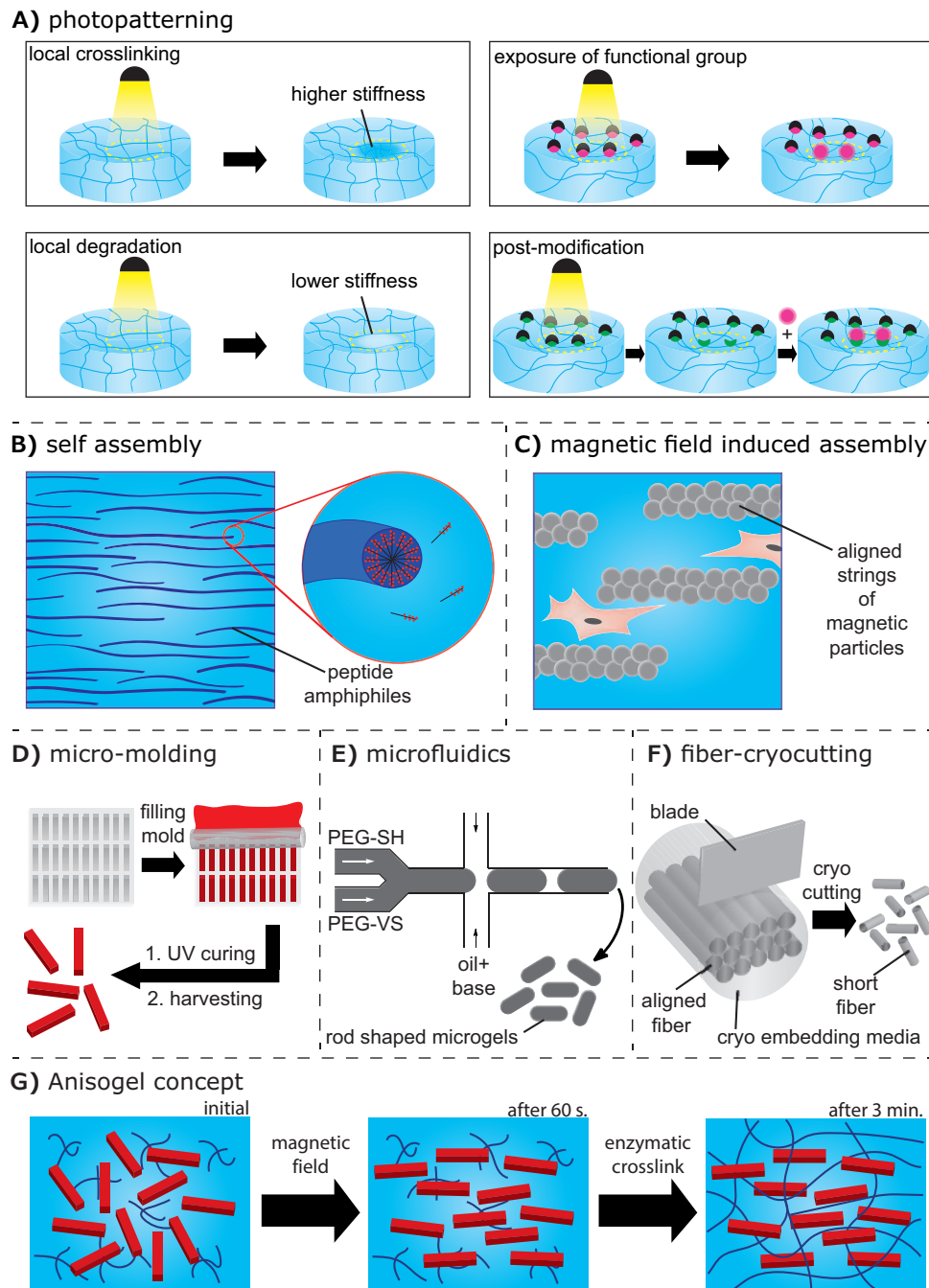


Figure 5. A) Photopatterning resulting in local crosslinking or degradation, exposure of functional groups, or post-functionalization. B) Self-assembly of peptide amphiphiles. C) Aligned strings of magnetic particles inside a hydrogel created by a magnetic field. D) In-mold polymerization method. E) Microfluidics for the preparation of rod-shaped microgels (star PEG-SH: star PEG-thiol and star PEG-VS: star PEG-vinylsulfone). F) Spinning/microcutting combinatorial method for short fiber production. G) Concept of the Anisogel.

within approximately 2–3 minutes. The elements can be rod-shaped microgels, produced either by in-mold polymerization or microfluidics, or short polymeric fibers, fabricated using a spinning/microcutting combinatorial method (Figure 5 D–F). The magneto-responsiveness is achieved by incorporating small amounts of superparamagnetic iron oxide nanoparticles (SPIONs) inside the micro-objects during fabrication. This technology allows for high degree of control over individual parameters like stiffness, bioactivity, topography, dimensions, and concentration of the guiding micro-elements, as well as the stiffness and bioactivity of the surrounding hydrogel (Figure 5G).¹⁸

Summary and Outlook

While most of the technologies described are still being developed and optimized, they allow for the identification of the factors that control cell behavior and tissue formation. These findings can be translated to organoids, which employ biopsy samples or stem cells to study the formation of mini-tissues, the onset of pathologies, and the effect of specific drugs (Figure 6). While Matrigel® is still the most efficient hydrogel material to create organoids, it is not well characterized, making a reductionist approach impossible.¹⁹ Therefore, synthetic approaches are under investigation to control and guide cell behavior in a more robust and reproducible manner.²⁰ While organoids are already a useful tool for *ex vivo* tissue models, they are still on the millimeter scale, limiting their use as implantable tissue engineering constructs for the replacement of damaged tissue. However, as our understanding grows of tissue

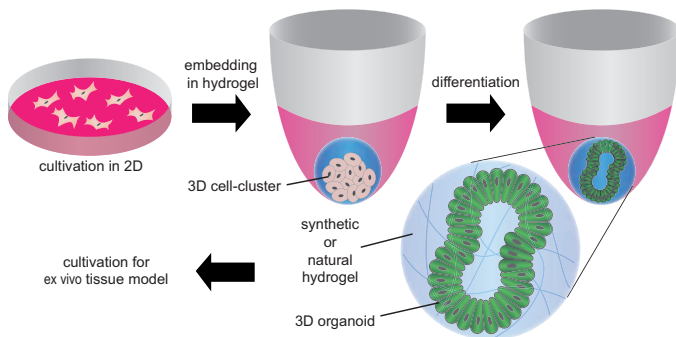


Figure 6. Formation of organoids by embedding stem cells in synthetic or natural hydrogels and differentiating/maturing them by using differentiation factors.

formation and the role of cell-ECM and cell-cell interactions during the stages of stem cell differentiation and maturation, these techniques hold promise for generating complex tissue constructs through natural organizational processes, without the need to guide each cell individually. By identifying the minimal amount of “outside” triggers required in an artificial environment, we may be able to target and activate natural healing and regeneration processes, which will be essential for generating entire organs in the future.

References:

- (1) Place, E. S.; Evans, N. D.; Stevens, M. M. *Nat. Mater.* **2009**, *8* (6), 457.
- (2) Ott, H. C.; Matthiesen, T. S.; Goh, S.-K.; Black, L. D.; Kren, S. M.; Netoff, T. I.; Taylor, D. A. *Nat. Med.* **2008**, *14* (2), 213.
- (3) Uygun, B. E.; Soto-Gutierrez, A.; Yagi, H.; Izamis, M.-L.; Guzzardi, M. A.; Shulman, C.; Milwid, J.; Kobayashi, N.; Tilles, A.; Berthiaume, F. *Nat. Med.* **2010**, *16* (7), 814.
- (4) Choudhury, M.; Mohanty, S.; Nayak, S. J. *Biomater. Tissue Eng.* **2015**, *5* (1), 1–9.
- (5) Sill, T. J.; von Recum, H. A. *Biomaterials* **2008**, *29* (13), 1989–2006.
- (6) Rose, J. C.; De Laporte, L. *Adv. Healthcare Mater.* **2018**, *7* (6), 1870026.
- (7) Torres-Rendon, J. G.; Femmer, T.; De Laporte, L.; Tigges, T.; Rahimi, K.; Gremse, F.; Zafarnia, S.; Lederle, W.; Ifuku, S.; Wessling, M. *Adv. Mater.* **2015**, *27* (19), 2989–2995.
- (8) Murphy, S. V.; Atala, A. *Nature Biotechnol.* **2014**, *32* (8), 773.
- (9) Moldovan, N. I.; Hibino, N.; Nakayama, K. *Tissue Eng. Part B Rev.* **2017**, *23* (3), 237–244.
- (10) Griffin, D. R.; Weaver, W. M.; Scumpia, P. O.; Di Carlo, D.; Segura, T. *Nat. Mater.* **2015**, *14* (7), 737–744.
- (11) (a) Hu, Y.; Mao, A. S.; Desai, R. M.; Wang, H.; Weitz, D. A.; Mooney, D. J. *Lab on a Chip* **2017**, *17* (14), 2481–2490; (b) Wang, H.; Hansen, M. B.; Löwik, D. W.; van Hest, J.; Li, Y.; Jansen, J. A.; Leeuwenburgh, S. C. *Adv. Mater.* **2011**, *23* (12), H119–H124.
- (12) Mealy, J. E.; Chung, J. J.; Jeong, H. H.; Issadore, D.; Lee, D.; Atluri, P.; Burdick, J. A. *Adv. Mater.* **2018**, 1705912.
- (13) (a) Kouwer, P. H.; Koepf, M.; Le Sage, V. A.; Jaspers, M.; van Buul, A. M.; Eksteen-Akeroyd, Z. H.; Woltinge, T.; Schwartz, E.; Kitto, H. J.; Hoogenboom, R. *Nature* **2013**, *493* (7434), 651; (b) Das, R. K.; Gocheva, V.; Hammink, R.; Zouani, O. F.; Rowan, A. E. *Nat. Mater.* **2016**, *15* (3), 318; (c) Jaspers, M.; Vaessen, S. L.; van Schayik, P.; Voerman, D.; Rowan, A. E.; Kouwer, P. H. *Nat. Commun.* **2017**, *8*, 15478.
- (14) Madl, C. M.; LeSavage, B. L.; Dewi, R. E.; Dinh, C. B.; Stowers, R. S.; Khariton, M.; Lampe, K. J.; Nguyen, D.; Chaudhuri, O.; Enejder, A. *Nat. Mater.* **2017**, *16* (12), 1233.
- (15) Cosgrove, B. D.; Mui, K. L.; Driscoll, T. P.; Caliani, S. R.; Mehta, K. D.; Asoian, R. K.; Burdick, J. A.; Mauck, R. L. *Nat. Mater.* **2016**, *15* (12), 1297.
- (16) (a) Kloxin, A. M.; Kasko, A. M.; Salinas, C. N.; Anseth, K. S. *Science* **2009**, *324* (5923), 59–63; (b) Mosiewicz, K. A.; Kolb, L.; Van Der Vlies, A. J.; Martino, M. M.; Lienemann, P. S.; Hubbell, J. A.; Ehrbar, M.; Lutolf, M. P. *Nat. Mater.* **2013**, *12* (11), 1072.
- (17) Zhang, S.; Greenfield, M. A.; Mata, A.; Palmer, L. C.; Bitton, R.; Mantei, J. R.; Aparicio, C.; De La Cruz, M. O.; Stupp, S. I. *Nat. Mater.* **2010**, *9* (7), 594.
- (18) Rose, J. C.; Cámara-Torres, M.; Rahimi, K.; Köhler, J.; Möller, M.; De Laporte, L. *Nano Lett.* **2017**, *17* (6), 3782–3791.
- (19) Dutta, D.; Heo, I.; Clevers, H. *Trends Mol. Med.* **2017**, *23* (5), 393–410.
- (20) Gjorevski, N.; Sachs, N.; Manfrin, A.; Giger, S.; Bragina, M. E.; Ordóñez-Morán, P.; Clevers, H.; Lutolf, M. P. *Nature* **2016**, *539* (7630), 560.

Natural Polymers for Tissue Engineering

Collagen

Name	Concentration	Endotoxin (EU/mL)	Cat. No.
Bovine Collagen Solution, Type I sterile filtered, BSE-Free, suitable for biomedical research	6 mg/mL	< 1.0	804622-20ML
Bovine Collagen Solution, Type I sterile filtered, BSE-Free, suitable for biomedical research	3 mg/mL	< 0.5	804592-20ML
Bovine Collagen Solution, Acid soluble telocollagen, Type I sterile filtered, BSE-Free, suitable for biomedical research	6 mg/mL	< 10	804614-20ML
Bovine fibrillar collagen solution, Type 1 % Denatured: ≤15% suitable for biomedical research	65 mg/mL	< 0.25	900721-1EA

ECM Gel

Name	Concentration	Cat. No.
ECM Gel from Engelbreth-Holm-Swarm murine sarcoma	8-12 mg/mL	E1270-1ML E1270-5ML E1270-10ML E1270-5X10ML
ECM Gel from Engelbreth-Holm-Swarm murine sarcoma, growth-factor reduced, without phenol red	7-9 mg/mL	E6909-5ML E6909-10ML

Fibrin

Name	Solubility	Cat. No.
Fibrin from human plasma, insoluble powder	25 mg in 1 mL 1 N NaOH	F5386-1G

Reagents for Solvent Casting

Name	Purity (%)	Description	Cat. No.
Sodium chloride	≥99.5 %	powder	S7653-250G S7653-1KG S7653-5KG
Potassium sodium tartrate tetrahydrate	≥99 %	powder	S6170-500G S6170-1KG
Sodium citrate monobasic	≥99.5 %	powder or crystals	71497-250G 71497-1KG

Synthetic Polymers for Hydrogels

Polyacrylamide

Name	Structure	Avg. M_n (Da)	Cat. No.
Polyacrylamide		40,000	738743-1G 738743-5G
		150,000	749222-5G 749222-25G

Poly(ethylene glycol)

Name	Structure	Avg. M_n (Da)	Cat. No.
4arm-PEG10K-Acrylate		10,000	JKA7068-1G
4arm-PEG10K-SH		10,000	JKA7008-1G
Acrylate-PEG3500-Acrylate		3,500	JKA4048-1G
Alkyne-PEG5K-Alkyne		5,000	JKA4095-1G
HS-PEG1500-SH		1,500	JKA4105-1G
Poly(ethylene glycol) diamine		6,000	752444-1G 752444-5G
Poly(ethylene glycol) diglycidyl ether		2,000	731811-5G

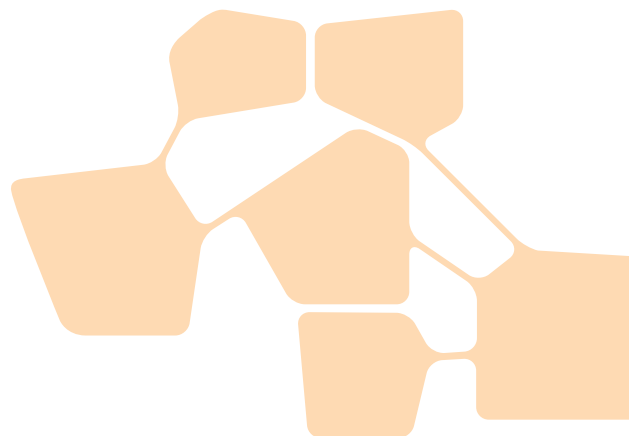
Poly(ethylene glycol) (PEG) and Synthetic PEG Derivatives for Tissue Engineering and Cell Delivery



Ali Affar, Fei Xu, and Todd Hoare*

McMaster University, Department of Chemical Engineering, 1280 Main Street West, Hamilton, Ontario, L8S 4L8, Canada.

*Email: hoaretr@mcmaster.ca



Introduction

Tissue engineering and regenerative medicine offers immense promise for improving and prolonging life, with several cell-based therapies now starting to reach the clinic. From functionally replacing entire organs to delivering therapeutic cells to an injured site, the success of any tissue engineering strategy is dependent on the biomaterial scaffold used to deliver and/or develop cells both *in vitro* and *in vivo*.¹ Successful tissue engineering scaffolds have several properties in common: (1) they must be reproducibly fabricated (part of the attractiveness of 3D printing strategies);² (2) they must be easy to deliver to the desired site of action, preferably via injection;^{1,3} (3) they should ideally match the physical and mechanical properties of the extracellular matrix (ECM) of the native tissue;⁴ (4) they must support the desired cell functionality, including adhesion, proliferation and/or differentiation;⁵ (5) they should induce minimal or no inflammatory response; and (6) they must degrade at an optimal rate into nontoxic byproducts that are generally regarded as safe for clearance by the body.

Hydrogels, are water-soluble polymer networks that are well-suited as tissue engineering scaffolds given their high water content, typically low inflammatory responses, tunable biomimetic mechanics, and highly variable chemistries. In particular, a wide variety of naturally occurring biopolymers such as polysaccharides, proteins, or nucleic acids (many of which can be found in the native ECM of cells) have been explored for use in tissue engineering applications.⁶ Biopolymers generally exhibit high cytocompatibility and can often degrade into safe extracellular matrix components like sugars and amino acids. However, the inherent bioactivity and the difficulty of reproducibly functionalizing such materials makes it difficult to control key properties such as degradation rate and mechanics.

Synthetic polymers can address these limitations since they can be engineered to produce hydrogels with well-defined chemistries, structures, mechanics, and residual functionalities. In particular, a synthetic approach allows for the incorporation of multiple functional moieties, including some that introduce “smart” properties such as *in situ* gelation, thermosensitivity, or pH-responsiveness, via typically facile copolymerization strategies.^{4,7} In some cases, synthetic polymers can also be tailored to degrade into small molecules; for example, the degradable polymer poly(lactide-co-glycolide) (PLGA) can degrade into the natural metabolites lactic acid and glycolic acid. However, there are fewer examples of water-soluble hydrogel precursor polymers with such functionality.⁴ Alternately, synthetic hydrogels can be developed to enable clearance by the renal system by controlling the polymer size and polydispersity and linking the polymers with degradable crosslinks.³

Among all reported synthetic polymers, poly(ethylene glycol) (PEG) has been the most extensively studied for tissue engineering. PEG offers the benefits of a hydrated structure, resulting in typically high cytocompatibility and protein repellency to minimize inflammatory responses.⁸ While the hydrophilicity of PEG makes it generally non-adhesive to cells, this can be overcome by incorporating cellular adhesive motifs such as arginylglycylaspartic acid (RGD) within the hydrogel.⁷ Based on these properties, PEG-based hydrogels have been successfully applied to a range of tissue engineering and cell delivery applications.⁹ However conventional PEG-based hydrogels are limited in terms of their lack of injectability, lack of tunable degradation, and relatively poor mechanics.

Herein, we describe how changing the crosslinking chemistry and/or the chain structure of the PEG starting materials can improve the performance of PEG and PEG-derivative hydrogels for tissue engineering or cell delivery applications.

Crosslinking Chemistry

Free radical polymerization of poly(ethylene glycol) diacrylates is the most common strategy for preparing PEG-based hydrogels, with the degree of crosslinking adjusted by changing the length of the PEG chain between the acrylate groups.¹⁰ However, the low swelling ratio, non-degradability, lack of injectability, and uncontrolled mesh size of the resulting hydrogels can create limitations in biomedical applications. Alternative crosslinking strategies have thus been designed to facilitate both injectability and degradability in PEG-based networks.

Injectability

To create injectable PEG-based hydrogels, the most common strategy is to co-extrude two PEG derivatives functionalized with complementary groups that can physically or chemically crosslink. Covalent *in situ* gelation, the more common of the two in tissue engineering, is enabled by converting the hydroxyl end group of PEG to a variety of rapidly reactive functional

groups to enable one or more of the various *in situ* crosslinking chemistries shown in **Figure 1**. By controlling the number, length, and reversibility of crosslinks formed, the physical properties of a hydrogel can be tuned.³

While all these chemistries have been applied successfully to various cell scaffolding applications, each has distinct advantages and drawbacks. Michael addition chemistry (**Figure 1A**) is relatively fast but creates a non-degradable linkage and can interact with proteins in the body. Disulfide formation (**Figure 1B**) yields redox-responsive hydrogels but is typically slower and yields weaker gels. Hydrazone chemistry (**Figure 1C**) is rapid and forms a hydrolyzable hydrazone bond but typically uses aldehyde groups that can form Schiff bases with amines in proteins. Oxime chemistry (**Figure 1D**) forms a more slowly degradable bond appropriate for longer-lasting scaffolds but requires acid catalysis for rapid gelation. Diels-Alder chemistry (**Figure 1E**) is highly bio-orthogonal but gels somewhat slowly and creates functionally irreversible crosslinks (at least without high temperatures). Strain-promoted alkyne/azide cycloaddition (**Figure 1F**) is rapid and highly specific but introduces significantly hydrophobicity into the hydrogel. Thus, the crosslinking chemistry must be chosen carefully in terms of balancing the gelation rate, the potential for side-reactions, and the rate of degradation most appropriate for each application.

Non-covalent interactions such as electrostatics, hydrogen bonding, stereocomplexation, or hydrophobic interactions can also be used to facilitate *in situ* gelation or create highly shear-thinning hydrogels that still enable injection.¹¹ However, these strategies often lead to hydrogels with poor stability in the highly diluted environment of the body and/or are subject to interferences *in vivo* that disrupt crosslinking. Inclusion complexes prepared using cyclic supramolecular structures like alpha-cyclodextrin (CD) as a host for polymers such as poly(ethylene glycol) do offer an interesting alternative though to covalent crosslinking.¹² Multiple PEG chains can thread through the center of the CD and interact via hydrogen bonding/dipole interactions to form a crosslinking point. Of particular relevance to tissue engineering, the mobility of the inclusion complex crosslinks (unlike covalent crosslinks) can lead to self-healing hydrogel structures. Combinations of covalent and non-covalent crosslinking strategies thus offer intriguing options that can address the drawbacks of both covalent and physical approaches. For example, Qiao et al. functionalized PEG with alkyne end-groups and CD rings with reactive azide groups to enabling both non-covalent (CD-PEG interactions) and covalent (alkyne/azide click chemistry) crosslinking (**Figure 2**). Both HeLa and HEK293T cells could be maintained inside the scaffold with greater than 90% viability over 10 days, and the gel can undergo complete degradation within 1 month.¹³

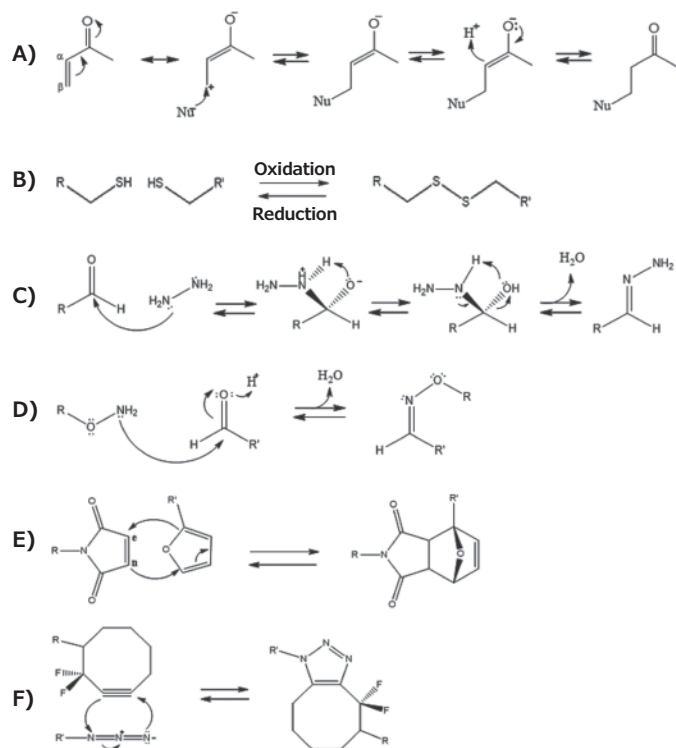


Figure 1. Examples of different *in situ* crosslinking chemistries: **A**) Michael addition; **B**) disulfide bond formation; **C**) hydrazone condensation; **D**) oxime formation; **E**) Diels-Alder cycloaddition; **F**) strain-promoted alkyne-azide Huisgen cycloaddition. (Reproduced with permission from reference 3, copyright 2014 John Wiley & Sons).

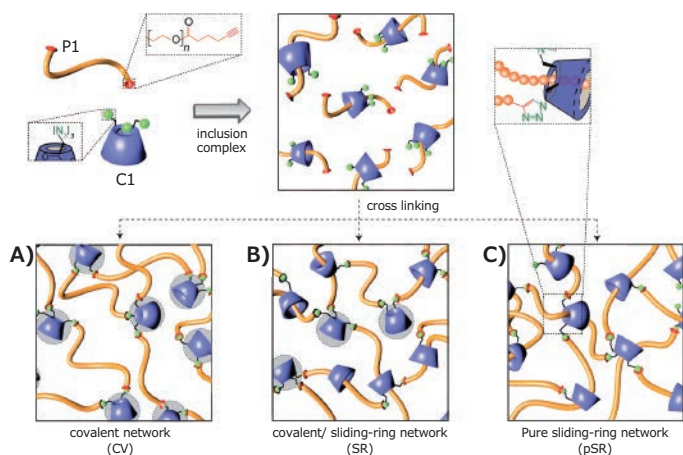


Figure 2. A schematic of the different network formation strategies applied in a hydrogel produced from alkyne-functionalized PEG and azide-functionalized CD. (Reproduced with permission from reference 13, copyright 2013 the Royal Society of Chemistry)

Degradability

To enable optimal tissue regeneration, the degradation rate of a scaffold should match the rate at which the cells inside propagate through the matrix and generate their own extracellular matrix, recreating native biology. Although common degradation mechanisms including hydrolysis may be engineered to enable such control, the use of specific stimuli such as light or disease state to dynamically degrade the gel under specific environmental conditions in which degradation is desirable is highly attractive.⁵

Enzymatic degradation is the most popular of these approaches, in which specific amino acid sequences that are substrates to various enzymes (including those specifically up-regulated in disease) are used as crosslinkers. The most commonly reported substrate is for matrix metalloproteases (MMPs), cell-secreted enzymes overexpressed in several inflammatory conditions and cancers.⁷ For example, Bryant et al. reported a PEG-based hydrogel loaded with pre-osteoblast cells and hydroxyapatite nanoparticles and crosslinked with MMP-sensitive peptide sequences; upon upregulation of MMPs during osteogenesis, the degradation rate of the hydrogel was accelerated to promote bone regeneration.⁹

UV or visible light have also been used to induce targeted degradation in hydrogels. Crosslinks can be manipulated by either light-induced *cis-trans* isomerization (e.g. azobenzenes or stilbenes) or reversible ring-opening/ring-closing isomerization (e.g. diarylethenes, spiropyrans, fulgimides) (Figure 3).⁵ Although such an approach is largely limited to *in vitro* use due to the low penetration of light through the body, it can be used in *in vivo* topical, dental, and optical implants to trigger photoinduced degradation events to either degrade or decrease the stiffness of the gel, the latter useful for promoting cell proliferation and/or inducing specific cell differentiation. For example, Anseth's group produced a cellularized hydrogel by crosslinking thiolated 4-armed star PEG and acrylate-functionalized poly(ethylene glycol) di-photodegradable acrylate (PEGdiPDA) via Michael addition chemistry and subsequently

degraded the hydrogel via cleavage of the *o*-nitrobenzyl ether photodegradable linker by UV irradiation.¹⁴ The on-demand switching of the hydrogel porosity and mechanics enabled precise control over cellular responses such as single stem cell migration¹⁵ and cell differentiation (e.g. the fibroblast-to-myofibroblast transition).¹⁶

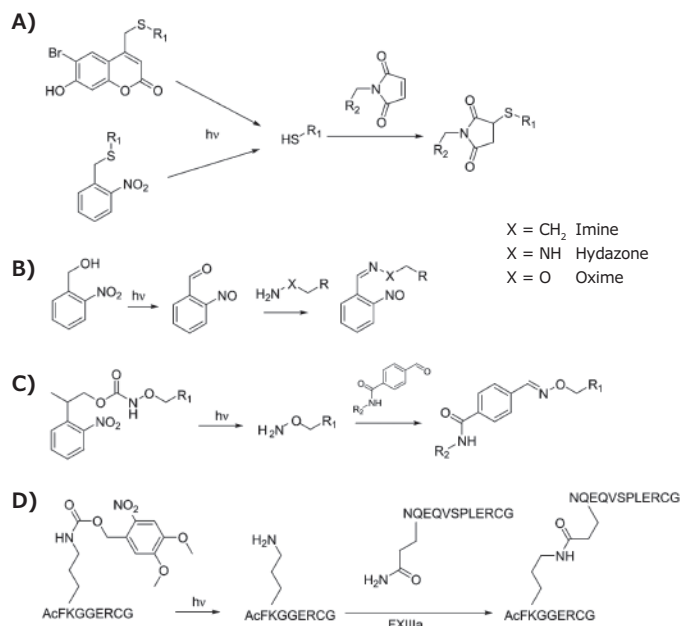


Figure 3. Four examples of photoresponsive crosslinking approaches. (Reproduced with permission from reference 5, copyright 2017 the Royal Society of Chemistry)

Chain Structure

The chemical structure of PEG and PEG-based derivatives plays an important role in regulating the hydrophilicity, biological responses, mechanical properties, protein repellency, degradation kinetics, and swelling of PEG-based hydrogels.¹⁷ Among the more common modifications made is to attach biodegradable hydrophobic polymer blocks based on polymers such as poly(lactic acid) (PLA), poly(lactide-co-glycolide) (PLGA), or poly(propylene oxide) (PPO) to PEG to form diblock or triblock copolymers that can self-associate into hydrogels via hydrophobic interactions but degrade over time as the hydrophobic polymer degrades.¹⁸ Triblock copolymers, particularly PEO-PPO-PEO (i.e. the Pluronics family of polymers), have been frequently investigated given their sol-gel transition behavior upon heating from room temperature to physiological temperature, which enables injection. For example, Kolesky et al. demonstrated the use of PEO-PPO-PEO as a thermogelling, cell-laden ink to create vascularized tissue constructs containing fibroblast cells by bioprinting.¹⁹ The susceptibility of these networks to dilution over time as well as their relatively poor mechanics limit such materials to use in engineering lower modulus tissues, although combining such polymers with covalent bond forming units (e.g. using diacrylated Pluronic F-127)²⁰ can in part address this drawback.

Changing the physical arrangement of the PEG chains from linear chains to more complex geometries also has significant impacts on gel properties. In particular, star or branched arrangements of PEG chains enable the formation of higher modulus and chemically tunable PEG hydrogels. This is due to the increasing number of crosslinkable groups per single chain compared to linear PEG, which has only one -OH group at each chain end.²¹ Spatially organizing PEG chains in the precursor materials also allows for the formation of more ordered and well-defined chemical structures, beneficial for promoting desirable cell responses.²²

Star PEG polymers are typically prepared by connecting 4, 6 or 8 arms of linear PEG (of tunable length) to a single internal point; the end group of each arm can be functionalized with biomolecules or crosslinkers as desired to create gels with more tunable mechanics and biological activities.²³ Indeed, tetrahedron-oriented 4-arm star PEGs have been shown to produce highly homogeneous network structures, enabling the production of hydrogels with moduli in the MPa range.²⁴ Star-PEGs can also be used in conjunction with injectable/degradable chemistries to form tissue scaffolds. For example, amphiphilic 8-armed PEG-*b*-PLA-cholesterol copolymers thermally gel at 34 °C due to interactions between the cholesterol groups to create a microstructured network that can support L929 mouse fibroblast cell viability and proliferation in the hydrogel.²⁵ Leveraging the additional surface functionality of star PEGs also allows for the creation of highly functional hydrogels without sacrificing crosslinking density. For example, RGD-modified star PEG coatings can significantly enhance cell spreading compared to non-RGD functionalized star PEG or RGD-functionalized linear PEG gels given the higher density of RGD that can be grafted using a star-PEG morphology.²⁶

To avoid the multiple-step synthesis of star PEGs, hyperbranched PEG copolymers (globular chains with molecular weights ranging from 1,400 g/mol to 1,700,000 g/mol) have been synthesized based on random anionic ring-opening copolymerization of ethylene oxide in the presence of glycidol.²⁷ This one-step free radical reaction method to create a PEG derivative with a high number of functionalizable chain ends is a synthetically and practically attractive, although it produces a more polydisperse starting unit than star PEGs (leading to weaker gels) and can result in low yields. To our knowledge, such materials have not yet been widely explored for tissue engineering applications.

Branched PEG copolymers offer an alternate and highly attractive option for creating PEG-based hydrogels. The most common branched PEG materials are based on poly(oligoethylene glycol methacrylate) (POEGMA), which consists of a methacrylate backbone and one PEG side chain of tunable length per monomer repeat unit.¹⁷ Such a structure offers facile polymerization via free or controlled radical processes enabling the formation of both linear and hyperbranched structures as well as easy functionalizability by copolymerization.²⁸ In addition, changing the length of the PEG side chain significantly changes the properties of the hydrogel. For example, Lutz and coworkers demonstrated that copolymerization of long side chain

oligo(ethylene glycol) methyl ether methacrylate (OEGMA) and short side chain di(ethylene glycol) methyl ether methacrylate (M(EO)₂MA) monomers leads to polymers and hydrogels with a precisely tunable lower critical solution temperature (LCST) between room temperature to >80 °C according to the ratio of OEGMA and M(EO)₂MA used.²⁹ LCST behavior converts the hydrogel from highly hydrophilic to somewhat hydrophobic, driving significant changes in cell adhesion and thus tunable cell delamination (Figure 4).³⁰

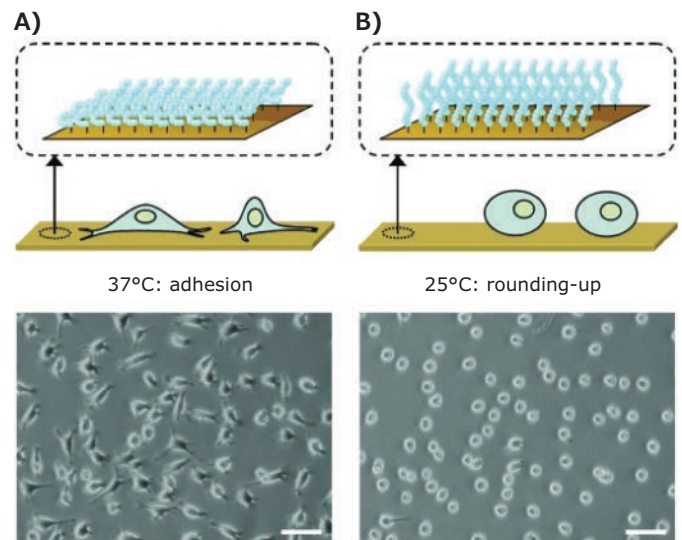


Figure 4. Microscopy images of L929 mouse fibroblasts on poly(OEGMA-co-M(EO)₂MA)-modified gold substrates after **A)** 44 hours at 37 °C and **B)** 25 °C for 30 mins. Scale bars = 100 μm. (Reproduced with permission from reference 30, copyright 2008 John Wiley and Sons).

Our lab has actively developed injectable or printable analogues of POEGMA hydrogels by functionalizing POEGMA precursor polymers with hydrazide and aldehyde reactive functional groups, enabling *in situ* gelation following mixing-based coextrusion via hydrazone crosslinking.³¹ The gelation time can be adjusted from minutes to hours for specific applications by changing the concentration, molecular weight, and/or density of reactive functional groups on the precursor polymers, enabling facile injection *in vivo* as well as processing via techniques like electrospinning to create well-defined nanofibrous hydrogel networks with the potential to mimic the nanofibrous extracellular matrix³² or ink jet printing to create immobilized hydrogel coatings on porous supports.³³ The PEG-based chemistry maintains low inflammatory responses upon injection *in vivo*, while the hydrazone gelation chemistry facilitates hydrolytic degradation over time; indeed, others have shown that branched PEGs can avoid some of the emerging immune responses observed with PEG-based materials.³⁴ In addition, the facile copolymerizability of POEGMA enables us to create a variety of functional POEGMA-based copolymers that are injectable while also introducing the potential for hydrophobic domain formation, temperature responsive swelling, cell delamination, or cell-adhesive properties, among others (Figure 5).¹⁷

In particular, from a cell delivery context, the introduction of charged groups by copolymerizing POEGMA with acrylic acid (AA, anionic charge) and/or *N,N*-dimethylaminoethyl methacrylate (DMAEMA, cationic charge) demonstrated significantly enhanced cell adhesion, with amphoteric hydrogels prepared by mixing cationic and anionic-functionalized precursor polymers in particular demonstrating improved cell viability for long-term encapsulation and delivery of retinal pigment epithelial cells to the back of the eye (Figure 6).³⁵

Conclusions

While the bio-inert nature of PEG has allowed PEG hydrogels to be used effectively in a variety of tissue engineering and cell delivery applications, the tunable chemical properties of PEG derivatives such as injectable and star/branched PEGs offer unique potential to control the chemistry, degradability, injectability, and mechanics of PEG-based hydrogels to improve their performance in cell-based applications. In particular, we believe the significantly improved chemical flexibility of PEG derivative hydrogels can address the inherent challenges of conventional PEG hydrogels, particularly in terms of improving the mechanics and cell-hydrogel interactions to direct desired tissue growth or cell differentiation/maintenance responses.

References

- (1) Liu, M.; Zeng, X.; Ma, C.; Yi, H.; Ali, Z.; Mou, X.; Li, S.; Deng, Y.; He, N. *Bone Res.* **2017**, *5*, 17014.
- (2) Kang, H.-W.; Lee, S. J.; Ko, I. K.; Kengla, C.; Yoo, J. J.; Atala, A. *Nat. Biotechnol.* **2016**, *34*, 312.
- (3) Patenaude, M.; Smeets, N. M. B.; Hoare, T. *Macromol. Rapid Commun.* **2014**, *35*, 598.
- (4) Khan, F.; Tanaka, M. *Int. J. Mol. Sci.* **2018**, *19*, 1.
- (5) Brown, T. E.; Anseth, K. S. *Chem. Soc. Rev.* **2017**, *46*, 6532.
- (6) Bedian, L.; Villalba-Rodríguez, A. M.; Hernández-Vargas, G.; Parra-Saldivar, R.; Iqbal, H. M. N. *Int. J. Biol. Macromol.* **2017**, *98*, 837.
- (7) Lu, Y.; Aimeetti, A. A.; Langer, R.; Gu, Z. *Nat. Rev. Mater.* **2016**, *2*, 16075.
- (8) Khoushabi, A.; Schmockler, A.; Pioletti, D. P.; Moser, C.; Schizas, C.; Månson, J. A.; Bourban, P. E. *Compos. Sci. Technol.* **2015**, *119*, 93.
- (9) (a) Skaalure, S. C.; Milligan, I. L.; Bryant, S. J.; Carles-Carner, M.; Saleh, L. S. *Biomed. Mater.* **2018**, *13*, 1. (b) Tan, S.; Blencowe, A.; Ladewig, K.; Qiao, G. G. *Soft Matter* **2013**, *9*, 5239. (c) Zhu, J. *Biomaterials* **2010**, *31*, 4639. (d) Wylie, R. G.; Ahsan, S.; Aizawa, Y.; Maxwell, K. L.; Morshead, C. M.; Shoichet, *Nat. Mater.* **2011**, *10*, 799.
- (10) (a) Sawhney, A. S.; Pathak, C. P.; Hubbell, J. A. *Macromolecules* **1993**, *26*, 581. (b) Revzin, A.; Russell, R. J.; Yadavalli, V. K.; Koh, W.-G.; Deister, C.; Hile, D. D.; Mellott, M. B.; Pishko, M. V. *Langmuir* **2001**, *17*, 5440.
- (11) Wang, Y.; Adokoh, C. K.; Narain, R. *Expert Opin. Drug Deliv.* **2018**, *15*, 77.
- (12) Poudel, A. J.; He, F.; Huang, L.; Xiao, L.; Yang, G. *Carbohydr. Polym.* **2018**, *194*, 69.
- (13) Tan, S.; Blencowe, A.; Ladewig, K.; Qiao, G. G. *Soft Matter* **2013**, *9*, 5239.
- (14) (a) Kloxin, A. M.; Kasko, A. M.; Salinas, C. N.; Anseth, K. S. *Science* **2009**, *324*, 59. (b) Tibbitt, M. W.; Kloxin, A. M.; Sawicki, L. A.; Anseth, K. S. *Macromolecules* **2013**, *46*, 2785.

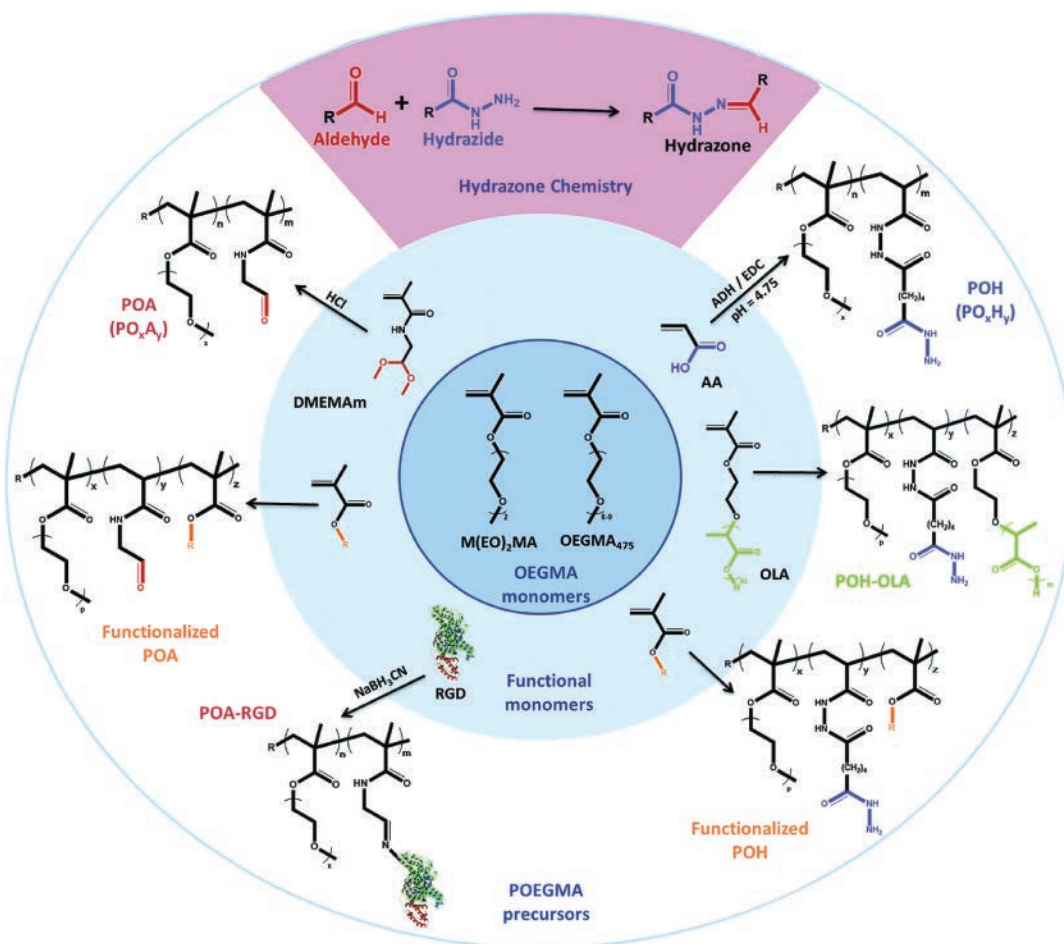


Figure 5. Library of functionalized hydrazone and aldehyde-functionalized poly(oligoethylene glycol methacrylate) (POEGMA) hydrogel precursors prepared via functional monomer copolymerization and/or post-polymerization grafting. (Reproduced with permission from reference 17, copyright 2015 Royal Society of Chemistry).

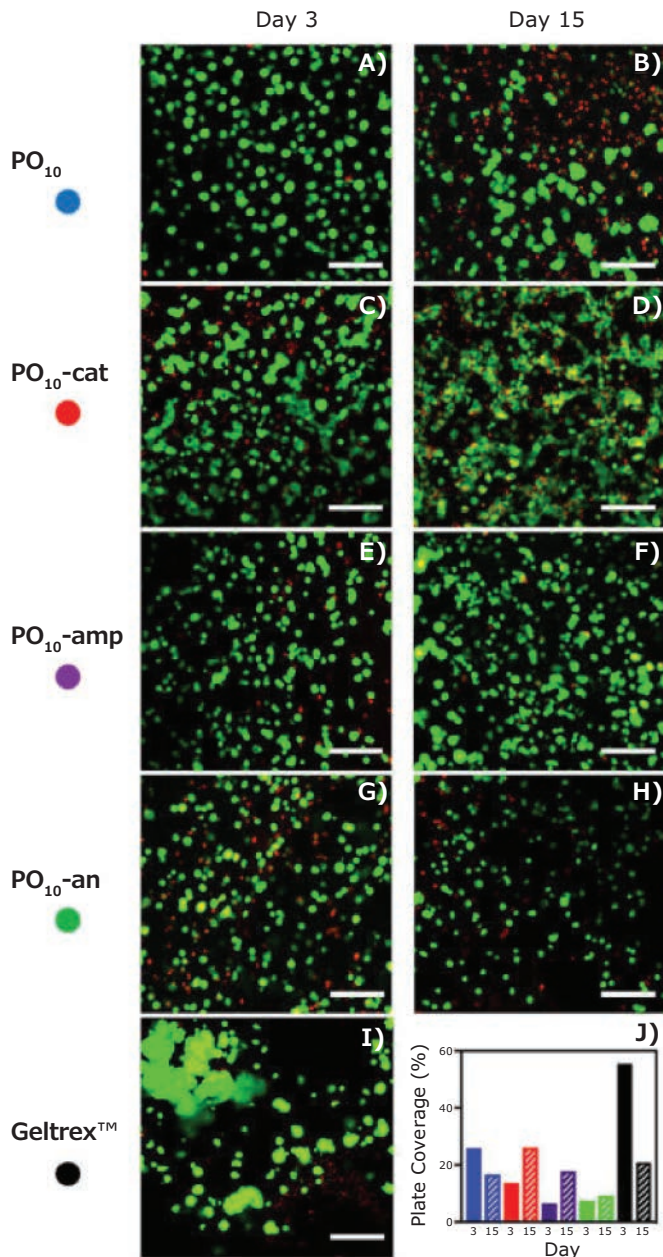
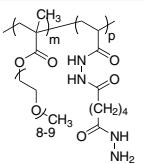
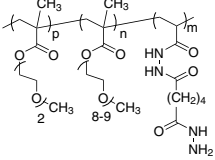
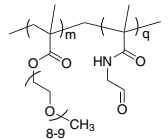
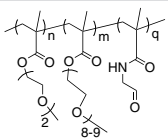


Figure 6. 3D encapsulation of ARPE-19 retinal epithelial cells imaged using confocal microscopy after 3 days and 15 days in (A, B) uncharged, (C, D) cationic, (E, F) amphoteric, and (G, H) anionic POEGMA injectable hydrogels compared to (I) a Geltrex™ matrix control. The percentage of fluorescence plate coverage of live cells for each gel and time point is shown in (J). Scale bar = 100 μ m. (Reproduced with permission from reference 35, copyright 2017 American Chemical Society).

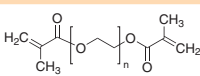
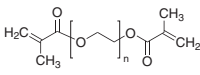
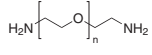
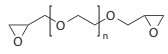
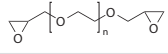
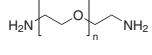
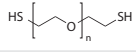
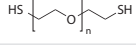
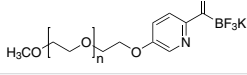
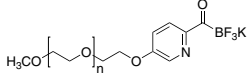
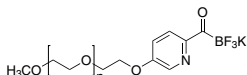
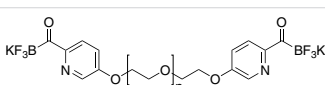
- (15) Guo, Q.; Wang, X.; Tibbitt, M. W.; Anseth, K. S.; Montell, D. J.; Elisseeff, J. H. *Biomaterials* **2012**, *33*, 8040.
- (16) Kloxin, A. M.; Benton, J. A.; Anseth, K. S. *Biomaterials* **2010**, *31*, 1.
- (17) Bakaic, E.; Smeets, N. M. B.; Hoare, T. *RSC Adv.* **2015**, *5*, 35469.
- (18) (a) Jeong, B.; Bae, Y. H.; Kim, S. W. *Macromolecules* **1999**, *32*, 7064. (b) Zhu, K.J.; Lin, X.; Yang, S. J. *Appl. Polym. Sci.* **2018**, *39*, 1.
- (19) Kolesky, D. B.; Truby, R. L.; Gladman, A. S.; Busbee, T. A.; Homan, K. A.; Lewis, J. A. *Adv. Mater.* **2014**, *26*, 3124.
- (20) Jin, Y. J.; Jung, C. H.; Gwan, P. T. J. *Biomed. Mater. Res. Part A* **2007**, *83A*, 597.
- (21) Keys, K. B.; Andreopoulos, F. M.; Peppas, N. A. *Macromolecules* **1998**, *31*, 8149.
- (22) Inoue, K. *Prog. Polym. Sci.* **2000**, *25*, 453.
- (23) Freudenberg, U.; Hermann, A.; Welzel, P. B.; Stirl, K.; Schwarz, S. C.; Grimmer, M.; Zieris, A.; Panyanuwat, W.; Zschoche, S.; Meinhold, D.; Storch, A.; Werner, C. *Biomaterials* **2009**, *30*, 5049.
- (24) Sakai, T.; Matsunaga, T.; Yamamoto, Y.; Ito, C.; Yoshida, R.; Suzuki, S.; Sasaki, N.; Shibayama, M.; Chung, U. *Macromolecules* **2008**, *41*, 5379.
- (25) Koji, N.; Tatsuro, O.; Yuichi, O. *Adv. Funct. Mater.* **2008**, *18*, 1220.
- (26) Groll, J.; Fiedler, J.; Engelhard, E.; Ameringer, T.; Tugulu, S.; Klok, H.-A.; Brenner, R.E.; Moeller, M. J. *Biomed. Mater. Res. Part A* **2005**, *74A*, 607.
- (27) (a) Perevyazko, I.; Seiwert, J.; Schömer, M.; Frey, H.; Schubert, U. S.; Pavlov, G. M. *Macromolecules* **2015**, *48*, 5887. (b) Wilms, D.; Schömer, M.; Wurm, F.; Hermanns, M. I.; Kirkpatrick, C. J.; Frey, H. *Macromol. Rapid Commun.* **2010**, *31*, 1811.
- (28) Luzon, M.; Boyer, C.; Peinado, C.; Corrales, T.; Whittaker, M.; Tao, L.; Davis, T.P. *J. Polym. Sci. Part A Polym. Chem.* **2010**, *48*, 2783.
- (29) (a) Lutz, J.-F.; Andrieu, J.; Üzgün, S.; Rudolph, C.; Agarwal, S. *Macromolecules* **2007**, *40*, 8540. (b) Lutz, J.-F.; Akdemir, Ö.; Hoth, A. *J. Am. Chem. Soc.* **2006**, *128*, 13046. (c) Lutz, J.-F. *Adv. Mater.* **2011**, *23*, 2237.
- (30) Wischerhoff, E.; Uhlig, K.; Lankeau, A.; Börner, H.G.; Laschewsky, A.; Duschl, C.; Lutz, J.-F. *Angew. Chemie Int. Ed.* **2008**, *47*, 5666.
- (31) (a) Bakaic, E.; Smeets, N. M. B.; Dorrington, H.; Hoare, T. *RSC Adv.* **2015**, *5*, 33364. (b) Smeets, N. M. B.; Bakaic, E.; Patenaude, M.; Hoare, T. *Chem. Commun.* **2014**, *50*, 3306.
- (32) Xu, F.; Sheardown, H.; Hoare, T. *Chem. Commun.* **2015**, *52*, 23.
- (33) Mateen, R.; Ali, M. M.; Hoare, T. *Nat. Commun.* **2018**, *9*, 602.
- (34) Liu, M.; Johansen, P.; Zabel, F.; Leroux, J.-C.; Gauthier, M. A. *Nat. Commun.* **2014**, *5*, 5526.
- (35) (a) Bakaic, E.; Smeets, N. M. B.; Badv, M.; Dodd, M.; Barrigar, O.; Siebers, E.; Lawlor, M.; Sheardown, H.; Hoare, T. *ACS Biomater. Sci. Eng.* **2017**, DOI: 10.1021/acsbomaterials.7b00397. (b) Bakaic, E.; Smeets, N. M. B.; Barrigar, O.; Alsop, R.; Rheinstädter, M. C.; Hoare, T. *Macromolecules* **2017**, *50*, 7687.

Functionalized POEGMA

Name	Structure	Avg. M_n (Da)	Concentration (wt%, aqueous)	Cat. No.
Poly(OEGMA), hydrazide functionalized		~20,000	25	901776-1G
Poly(M(EO) ₂ MA:Poly(OEGMA) 90:10, hydrazide functionalized		~20,000	25	901546-1G
Poly(OEGMA), aldehyde functionalized		~20,000	25	901743-1G
Poly(M(EO)2MA:Poly(OEGMA), (90:10), aldehyde functionalized		~20,000	25	901777-1G

Functionalized Poly(ethylene glycol)

Linear

Name	Structure	Avg. M_n (Da)	Cat. No.
Poly(ethylene glycol) dimethacrylate		2,000	687529-1G
		6,000	687537-1G
Poly(ethylene glycol) diamine		2,000	753084-1G 753084-5G
Poly(ethylene glycol) diglycidyl ether		2,000	731811-5G
		1,000	805505-5G
Poly(ethylene glycol) diamine		3,000	752452-1G 752452-5G
Poly(ethylene glycol) dithiol		1,500	704369-1G
		3,400	704539-1G
Methoxy poly(ethylene glycol) KAT		20,000	901645-500MG
		5,000	901644-500MG
		10,000	901642-500MG
Poly(ethylene glycol) bis(2-pyridyl) KAT		10,000	901635-500MG

Multi-arm

Name	Structure	Avg. M_n (Da)	Cat. No.
4arm-PEG10K-Acrylate		10,000	JKA7068-1G
4arm-PEG10K-NH ²		10,000	JKA7011-1G
4arm-PEG10K-COOH		10,000	JKA7027-1G
4arm-PEG10K-Vinylsulfone		10,000	JKA7005-1G
4arm-PEG10K-SH		10,000	JKA7008-1G
4arm-PEG20K-Isocyanate		20,000	JKA7111-1G
4arm-PEG20K-Acrylate		20,000	JKA7034-1G
4-arm-PEG10K-KAT		10,000	901637-500MG
4arm-PEG20K-NH ₂		20,000	JKA7026-1G

MilliporeSigma
400 Summit Drive
Burlington, MA 01803

Materials Matter

Your partner in materials innovation.

Find out more on
SigmaAldrich.com/materials-synthesis

**"...because innovative
materials start with
innovative chemistry."**

Millipore
Sigma



© 2018 Merck KGaA, Darmstadt, Germany and/or its affiliates. All Rights Reserved. MilliporeSigma and the sigma M are trademarks of Merck KGaA, Darmstadt, Germany or its affiliates. All other trademarks are the property of their respective owners. Detailed information on trademarks is available via publicly accessible resources.
US No. MO_982492N 2018-14439 12/2018

The life science business
of Merck KGaA,
Darmstadt, Germany
operates as MilliporeSigma
in the U.S. and Canada.

Sigma-Aldrich®
Lab & Production Materials